NASA/CR—2003-212194

Modeling of High-Strain-Rate Deformation, Fracture, and Impact Behavior of Advanced Gas Turbine Engine Materials at Low and Elevated Temperatures

Mostafa Shazly, David Nathenson, and Vikas Prakash
Case Western Reserve University, Cleveland, Ohio

May 2003

The NASA STI Program Office . . . in Profile

Since its founding, NASA has been dedicated to the advancement of aeronautics and space science. The NASA Scientific and Technical Information (STI) Program Office plays a key part in helping NASA maintain this important role.

The NASA STI Program Office is operated by Langley Research Center, the Lead Center for NASA's scientific and technical information. The NASA STI Program Office provides access to the NASA STI Database, the largest collection of aeronautical and space science STI in the world. The Program Office is also NASA's institutional mechanism for disseminating the results of its research and development activities. These results are published by NASA in the NASA STI Report Series, which includes the following report types:

- TECHNICAL PUBLICATION. Reports of completed research or a major significant phase of research that present the results of NASA programs and include extensive data or theoretical analysis. Includes compilations of significant scientific and technical data and information deemed to be of continuing reference value. NASA's counterpart of peer-reviewed formal professional papers but has less stringent limitations on manuscript length and extent of graphic presentations.

- TECHNICAL MEMORANDUM. Scientific and technical findings that are preliminary or of specialized interest, e.g., quick release reports, working papers, and bibliographies that contain minimal annotation. Does not contain extensive analysis.

- CONTRACTOR REPORT. Scientific and technical findings by NASA-sponsored contractors and grantees.

- CONFERENCE PUBLICATION. Collected papers from scientific and technical conferences, symposia, seminars, or other meetings sponsored or cosponsored by NASA.

- SPECIAL PUBLICATION. Scientific, technical, or historical information from NASA programs, projects, and missions, often concerned with subjects having substantial public interest.

- TECHNICAL TRANSLATION. English-language translations of foreign scientific and technical material pertinent to NASA's mission.

Specialized services that complement the STI Program Office's diverse offerings include creating custom thesauri, building customized databases, organizing and publishing research results . . . even providing videos.

For more information about the NASA STI Program Office, see the following:

- Access the NASA STI Program Home Page at ***http://www.sti.nasa.gov***

- E-mail your question via the Internet to help@sti.nasa.gov

- Fax your question to the NASA Access Help Desk at 301–621–0134

- Telephone the NASA Access Help Desk at 301–621–0390

- Write to:
  NASA Access Help Desk
  NASA Center for AeroSpace Information
  7121 Standard Drive
  Hanover, MD 21076

NASA/CR—2003-212194

Modeling of High-Strain-Rate Deformation, Fracture, and Impact Behavior of Advanced Gas Turbine Engine Materials at Low and Elevated Temperatures

Mostafa Shazly, David Nathenson, and Vikas Prakash
Case Western Reserve University, Cleveland, Ohio

Prepared under Grant NAG3–2677

National Aeronautics and
Space Administration

Glenn Research Center

May 2003

Acknowledgments

The authors would like to acknowledge financial support from NASA's advanced aeropropulsion research program through NASA Grant NAG3–2677. The authors would also like to thank Dr. Susan Draper of NASA GRC and Andreas Venskutonis of Plansee, Austria, for providing the Gamma Met PX material used in the present study. The authors would also like to thank Dr. J.M. Pereira for several helpful technical discussions. The authors would also like to acknowledge the financial support from the National Science Foundation through grants CMS–9908189 and CMS–0079458 in setting up part of the elevated temperature and high-speed imaging facility at CWRU.

This report contains preliminary findings, subject to revision as analysis proceeds.

The Propulsion and Power Program at NASA Glenn Research Center sponsored this work.

Available from

NASA Center for Aerospace Information
7121 Standard Drive
Hanover, MD 21076

National Technical Information Service
5285 Port Royal Road
Springfield, VA 22100

Available electronically at http://gltrs.grc.nasa.gov

INTRODUCTION

Advanced intermetallics, such as cast gamma titanium-aluminides (γ-TiAl), are considered to be one of the leading candidate materials for aircraft propulsion systems. When compared with Ni-based superalloys, γ-TiAl alloys are known to have lower density, excellent high-temperature strength retention, high specific stiffness at elevated temperatures, and good oxidation and corrosion resistance. However, these alloys have low ductility and poor crack-propagation resistance. As a result, in contemplating the use of γ-TiAl in airfoils, the threat of high velocity particle impact has always been of considerable concern to designers.

In view of the stringent safety requirements of modern aero-propulsion systems and our incomplete state of understanding of the fundamental mechanisms involved during deformation and fracture of γ-TiAl alloys under impact loading conditions, a three-year integrated experimental, analytical, and computational program of research is being conducted at CWRU. During the first two year time period the focus of the research work will be to better characterize the dynamic material behavior of γ-TiAl alloys under impact loading conditions. The dynamic material properties of interest include, (a) dynamic compressive and tensile strength as a function of strain rate ranging from 100 s^{-1} to 10^4 s^{-1} and temperatures ranging from room to 900 °C, (b) dynamic fracture characteristics, including dynamic fracture toughness and ductile-to-brittle transition as a function of crack-tip loading rates, and (c) high-velocity particle-impact experiments to understand the initiation and spread of damage including micro- and macro-cracking and development of spall in γ-TiAl. In these later experiments the variables of primary interest include energy (impact velocity), specimen thickness, hardness of the projectile, and test temperatures.

Two full-time graduate students are directly involved on the project: Mostafa Shazly and David Nathenson. Mostafa Shazly has completed his MS and is working towards his Ph.D. while David Nathenson is currently working on MS and will continue on his Ph.D.

Accomplishments during the first year:

- *Design and development of elevated temperature facility to conduct high-strain rate experiments at elevated temperatures.* This high-temperature facility has been designed and built and integrated with the Split Hopkinson pressure bar apparatus to conduct elevated temperature high-strain-rate experiments on γ-TiAl in both compression and tension. To-date elevated temperature high-strain-rate tests on gamma Met PX have been conducted in compression and tension at strain rates varying from 100/s to 3000/s and temperatures ranging from room to 900 °C.

- *Design and development of gas-gun facility for accelerating 1/16 to 1/8 inch projectiles for conducting high-velocity particle impact experiments.*

A more detailed description of the accomplishments during the first year is described next.

HIGH STRAIN RATE DEFORMATION OF GAMMA-MET PX AT ELEVATED TEMPERATURES

Graduate Student: Mostafa Shazly

Although the introduction of classical titanium alloys such as IMI-834 and Ti-1100, have allowed improvements in the efficiency of gas turbine engines by replacing nickel and iron base superalloys, they cannot still meet the requirements of high operating temperatures and high specific strength of modern air-breathing propulsion systems. This is because at temperatures over 600 °C the mechanical strength and creep behavior of titanium alloys becomes inadequate. Moreover, oxidation problems arise due to the formation of brittle oxide surface layer, which leads to premature fracture damage in fatigue. Also, these alloys are subject to "titanium fire" (a great problem for engine applications), a phenomenon that results from the low thermal conductivity of the metal and the very high heat of formation of TiO_2 oxide (Young-Won Kim, 1989; Djanarthany, Viala and Bouix, 2001).

Gamma titanium aluminides (γ-TiAl) are targeted as a material substitute for superalloys (LeHolm, Clemens and Kestler, 1999) for critical propulsion components in the 600 to 900 °C temperature range. Compared with titanium alloys, they present several advantages such as higher elasticity modulus, lower density, better mechanical behavior with temperature and higher oxidation resistance by formation of a surface passive alumina layer. However, these properties come at the expense of tensile ductility, which is typically in the range of 1 to 3%. As a result these intermetallics show poor crack-propagation resistance, and in contemplating the use of γ -TiAl in airfoils the threat of high-velocity small particle impacts is of considerable concern to designers (Wright, 1993; Austin, Kelly and McAllister, 1997). The absence of plasticity at classical fabrication temperatures is also a source of difficulty, in particular, in rolling γ-TiAl into thin sheets or foils.

Gamma based titanium aluminides have an aluminum level of 45-52 at.%. Within this regime, there are two phases of interest-- the γ-TiAl ordered phase with face center tetragonal (f.c.t) $L1_0$ crystal structure with alternating (002) planes of Ti and Al atoms (Lui and Stiegler, ; Young-Won Kim, 1989; Dimiduk *et al.*, 1991; Kim and Dimiduk, 1991; Yamagushi, 1993; Recina, 2000; Djanarthany, Viala and Bouix, 2001), and ordered α_2-Ti_3Al phase with the DO_{19} hexagonal close packed (h.c.p) crystal structure. α_2 -Ti_3Al contains three linearly independent slip systems that account for dislocation motion on the basal {0001}, prism {1010}, and pyramidal {0221} planes (Lui and Stiegler,). Pure γ remains ordered up to the melting point of 1440 °C, while the α_2 transforms at around 1125 °C to a disordered h.c.p structure (Recina, 2000). Because they have slower diffusion rates than conventional titanium alloys, titanium aluminides feature enhanced high-temperature properties such as strength retention, creep and stress rupture, and fatigue resistance (Lui and Stiegler, ; Millett, Gray and Bourne, 2000). In improving the mechanical properties of gamma titanium aluminides, Plansee AG of Austria has developed new generation of gamma titanium called Gamma Met. Gamma Met is available in both sheet and rod forms. This product is unique, because it is suitable for both propulsion and airframe components. Moreover, Gamma Met has better rolling characteristics and improved post-rolling mechanical properties. It does not need the costly fabrication processes typically used for other intermetallic components. Shaping and forming can be carried out at relatively low temperatures to produce parts which are more uniform than those obtained with other methods. Components can be economically fabricated in normal production settings with the same equipment as that used for conventional titanium alloys. In summary the main advantages of γ-Met material are (a) γ-Met

alloy is 15% lighter than titanium alloys and more than 50% lighter than superalloys, (b) it withstands temperatures that are approximately 300°C higher than those for titanium alloys, (c) its specific stiffness is approximately twice that of titanium alloys and superalloys (based on modulus normalized with respect to density), (d) it exhibits high acoustic attenuation due to high specific stiffness, and (e) fabrication costs associated with γ-Met alloys are potentially the same as for titanium alloys and superalloys (Venskutonis, 2000).

In the past little work has been done in the area of high-strain-rate deformation of γ-TiAl at elevated temperatures. Maloy and Gray III (1996) studied the high strain rate properties of duplex microstructures of Ti-48Al-2Cr-2Nb in compression. Their study showed that Ti-48-2-2 has a yield stress anomaly at approximately 600°C. However, in the work of Gardiner et al. (1997) on duplex microstructures of Ti-38.5Al-2.7Nb-2.6Mn, no yield-stress anomaly was observed. The material showed strain hardening at all levels of plastic strain and test temperatures. Moreover, thermal softening was observed as the test temperature was increased above the room temperature. In tests performed between 700°C and 800°C and at strain rates of approximately 2500 s^{-1}, cracking and fracture was observed at macroscopic plastic strains of 0.32. However, at temperatures below 700°C and similar strain rates no macro- and/or micro- cracking was observed.

Wang et al (1999a) studied the high-strain-rate tensile properties of both duplex and fully lamellar microstructures of Ti-47Al-1.5Cr-.5Mn-2.8Nb at room temperature. Contrary to the observations of Maloy and Gray III (1996), they showed that the strength of duplex microstructures of Ti-48-2-2 decreases with increasing strain rate. However, for fully lamellar microstructure the material showed increasing strength with increasing strain rates. In another work by Wang et al. (1999b) on nearly lamellar microstructures of Ti-47Al-2Mn-2Nb, the material was observed to show increasing strength with increasing strain rate.

The objective of our present work is to understand the high-strain-rate compression behavior of Gamma Met PX alloy (developed by GKSS of Germany), at temperatures ranging from room to 900 °C and strain rates ranging from quasi-static to 3500 s^{-1}. The report describes the development of the SHPB and SHTB facilities to conduct the elevated temperature experiments and the results of high-strain-rate uniaxial compression/tension tests on Gamma Met PX.

EXPERIMENTAL WORK

MATERIAL

Gamma Met PX has a chemical composition of Ti-45Al-X(Nb, B, C). The material used in the present study was supplied by Plansee AG in the form of ½" rods. The material was VAR cast and then hot extruded above the alpha transus temperature. The extrusion ratio was 100:1 and the bars are in the as-extruded condition. Microstructural investigation, Figure 1, shows that the material consists of nearly lamellar microstructure. The nearly lamellar microstructure was chosen since it has been shown to provide these alloys with high strength and acceptable levels of ductility (Kim, 1989; Dimiduk *et al.*, 1991; Kim and Dimiduk, 1991).

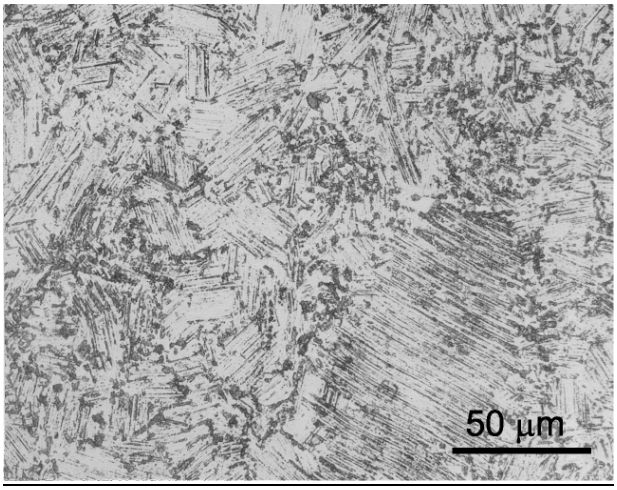

Figure 1: Microstructure of the as received Gamma Met PX.

DYNAMIC COMPRESSION TESTS: SPLIT HOPKINSON PRESSURE BAR (SHPB)

Typical screw driven or servo-hydraulic testing machines are routinely utilized to obtain mechanical properties of engineering materials at strain rates less than $1s^{-1}$. High capacity servo-hydraulic testing machines with high speed valves, control, and data acquisition instrumentation, can be used during compression testing to achieve strain rates as high as 100 s^{-1}. However, to achieve higher strain rates (as high as 10,000 s^{-1}), a split Hopkinson pressure bar (SHPB) is commonly employed. The historical prospective and the development of SHPB can be found elsewhere (Follansbee, 1985; Kaiser, 1998; Gray, 2000). The classical SHPB consists of two long bars with high elastic limit, termed incident and transmitted bars respectively, sandwiching a small cylindrical specimen, and a striker bar as shown in Figure 2.

The SHPB facility at CWRU comprises of striker, incident and transmitted bars that are made from 19.05 mm diameter maraging steel having nominal yield strength of 2500 MPa. The striker bar is approximately 0.508 m long and the incident and transmitted bars are 1.524 m long. The striker bar is accelerated using an air operated gas gun. A pair of strain gages (Measurements Group WK-06-250BF-10C) are strategically attached on each of the incident and transmitted bars and are used in combination with a Wheatstone bridge circuit connected with a differential amplifier (Tektronix 5A22N) and a digital oscilloscope (Tektronix TDS 420) to monitor the strain during the test. When the striker bar hits the incident bar, a compressive pulse travels along the incident bar, and called the incident wave ε_i. When the incident pulse reaches the specimen/bar interface, a reflected pulse ε_r, travels back along the incident bar and a transmitted pulse ε_t, travels through the specimen to the transmitter bar.

For determination of the dynamic flow characteristics of Gamma Met PX, cylindrical compression tabs (4.70 mm diameter by 2.35 mm thick) were machined from a 12.7 mm diameter bar. The relatively small size of the specimens allow a stress amplification (ratio of stress in the sample to stress in bar) of 16:1, which was found to be necessary to deform the Gamma Met PX alloy specimens at high strain rates in view of the high yield-stress of Gamma Met PX alloy. Prior to the tests the two lateral surfaces (faces) of the specimens were ground and lapped flat.

For the room temperature experiments Molybdenum grease was applied liberally in order to prevent friction at the specimen/bar interface.

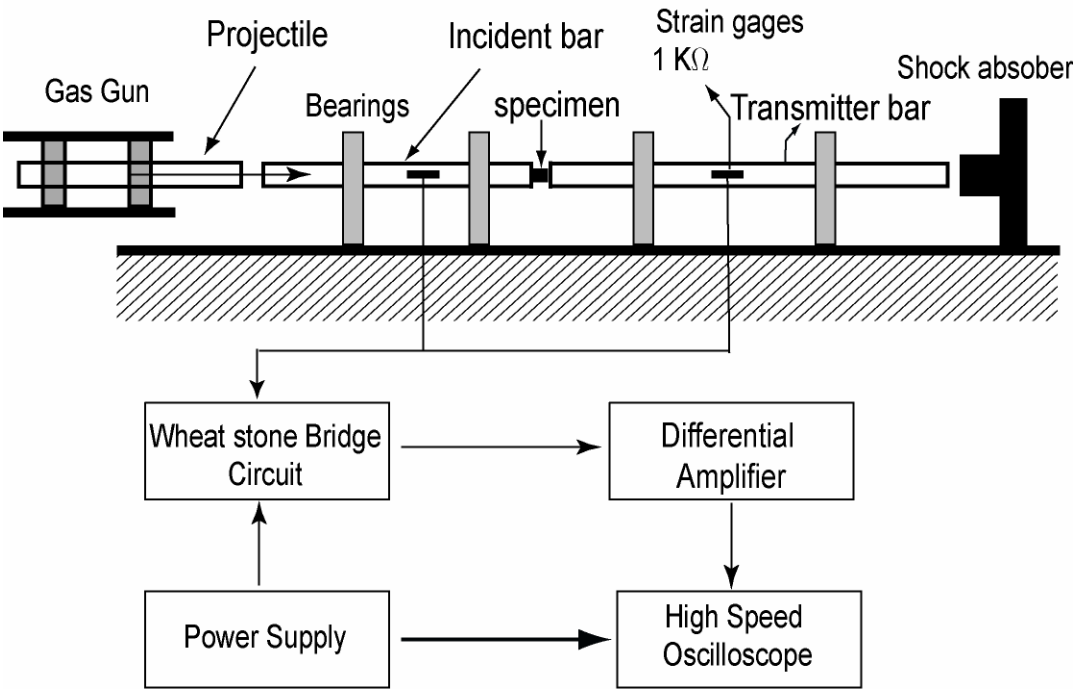

Figure 2: Schematic of Split-Hopkinson Bar at Case Western Reserve University.

The theory behind SHPB is based on one dimensional elastic wave propagation in slender bars. According to superposition of one-dimension wave and homogeneity of stress and strain in the specimen, the expressions for strain ε(t), strain rate $\dot{\varepsilon}$(t), and stress σ(t) in the specimen are given as (Follansbee, 1985)

$$\varepsilon(t) = \int_0^t \dot{\varepsilon}(\tau)\, d\tau\,, \tag{1}$$

$$\dot{\varepsilon}(t) = \frac{2C_b\varepsilon_r}{l_s}\,, \tag{2}$$

$$\sigma(t) = \frac{AE\varepsilon_t}{A_s}\,, \tag{3}$$

where C_b, is the longitudinal wave speed of the stress wave in the bar, A is the cross sectional area, and E is the Young's modulus of the bar, and l_s and A_s are the length and cross sectional area of the specimen, respectively.

HIGH TEMPERATURE TESTING SET-UP FOR SHPB

Determination of dynamic response of a material at elevated temperatures using the SHPB is a challenging task. This is primarily due to the fact that heating the specimen while in contact with the bars also results in heating the ends of the incident and transmitter bars. This leads to a temperature gradient in the two bars, which in turn affects the elastic modulus and the density of the pressure bars, both of which are known to vary with temperature. Thus, in order to obtain accurate stress-strain curves, a correction needs to be applied to the strain-gage signals to compensate for the temperature dependent longitudinal wave velocity and elastic modulus by estimating the temperature gradient in the bars. Another problem of heating the specimen alone and then bringing the bars in contact, is the cold contact time. As soon as the bars come in contact with the specimen, the specimen loses its temperature by heat conduction to the bars. Figure 3 shows a finite element simulation of heat conduction in the specimen and the bar assembly using the commercial FEM package ABAQUS™ (2001). The analysis shows that the temperature distribution within the specimen changes continuously as soon as the bars are brought in contact.

Several approaches have been used in the past to alleviate these problems. Amongst them an approach based on mechanical devices is to bring the bars in contact with the specimen just before the arrival of the pulse at the specimen plane has found wide spread use (see for example Frantz et al. (1984) and Lennon and Ramesh (1998). However, controlling the time between bringing the bars in contact and the arrival of the pulse is critical and even with the smallest contact time the temperature along the specimen is not uniform as shown in Figure 3. Other methods include, the use of Inconel 718 bars in testing up to 600 °C, as they retain their elastic properties up to this temperature, and the use of long aluminum oxide bars in contact with the steel bars for testing up to 1500 °C (Follansbee, 1985).

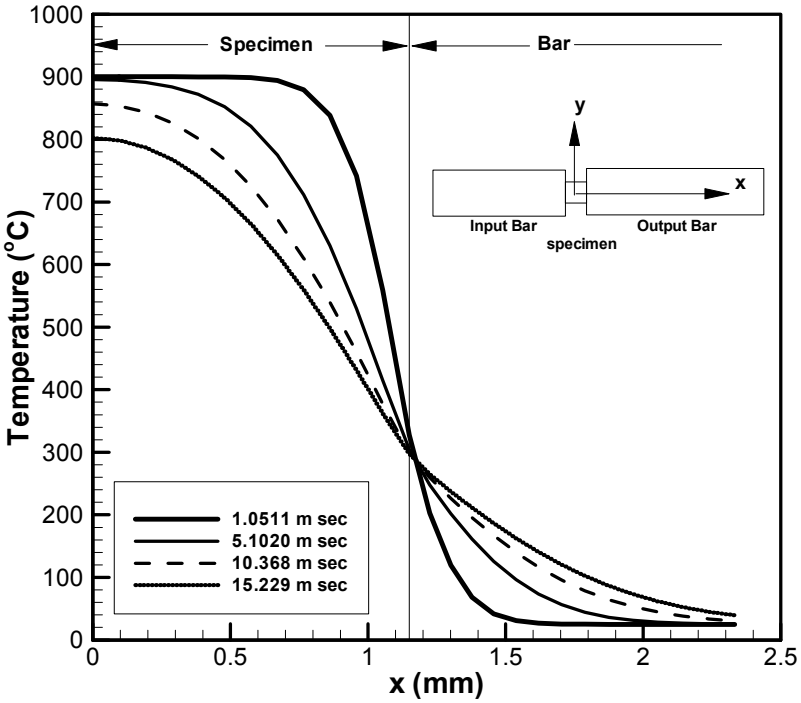

Figure 3: Temperature distribution in the specimen as a function of time after the specimen is brought in contact with the bars.

The schematic layout of the high temperature tests set up at CWRU is shown in Figure 4. In addition to the conventional SHPB, two air-cooled infrared spot heaters are used as the heating elements. The IR spot heaters have a circular cut shield which concentrates the heat flux at the focal point (0.25 inch diameter) as high as 650 watts per square inch. In order to overcome the problem of cold contact times between the bars and the specimen and thus allow sufficient time for the movement of the bars, the specimen is sandwiched between two WC inserts and the assembly comprising the inserts and the specimen is heated to the desired test temperature. The WC inserts are impedance matched to the incident and the transmitter bars, and hence do not disturb the incident, reflected and the transmitted wave profiles.

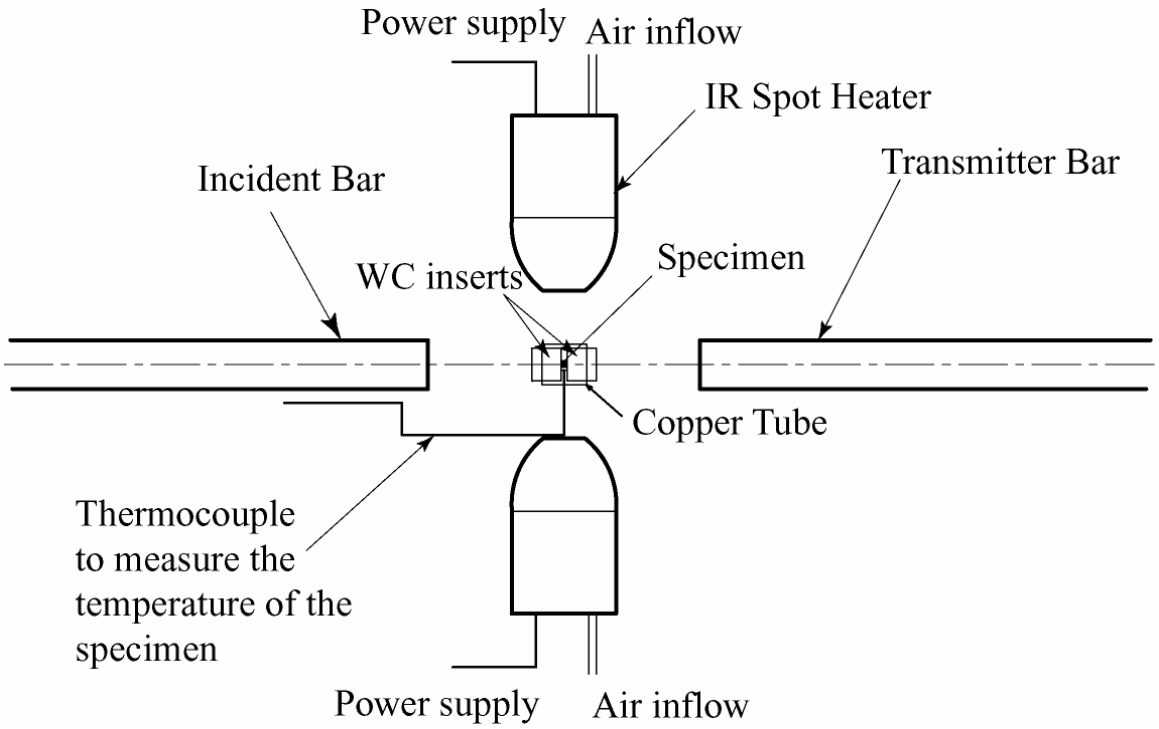

Figure 4: Schematic of the high temperature set-up used in the present investigation.

Just prior to conducting the test, the insert-specimen-insert assembly is heated up to the desired temperature level (usually 50 to 100 °C higher than the test temperature), and then the bars are brought manually in contact with the assembly. The specimen is being held between the two inserts by thermocouple wires pre-deformed to a cup-shape. This allows a near free expansion of the specimen during the compression test. The cup-shaped wires are spot welded to a screw that move inside a T-shape copper tube. The T-shape copper tube supports the WC inserts and allows for precise alignment with the incident and transmitter bars, as shown in Figure 5. A 0.015" chromel-alumel wire is spot welded to the specimen to monitor the specimen temperature prior to the test. This allows testing to be carried out over the range from room to 1000 °C. For high temperature experiments, boron nitride was used as lubricant agent between the specimen-inserts interfaces as well as the inserts-bars interfaces.

When the bars make contact with the specimen, the WC inserts loose heat to the bars while maintaining the specimen temperature at the desired level for a long enough time-period so as to

allow the test to be conducted at nominally uniform temperature conditions within the specimen. A finite element model for the set-up is shown in Figure 6. From the plot we see that for a test to be conducted at 800 °C, an initial temperature of 900 °C of the specimen and the WC insert assembly allows approximately 6.5 seconds to conduct the experiment before a temperature gradient develops within the specimen. The temperature remains fairly uniform along the entire length of the specimen during this time interval. However, in actual tests longer times to conduct the experiments are available because of the presence of the high temperature lubricant layer between the WC inserts which essentially acts as a thermal barrier, and the fact that the IR spot heaters were left on until just prior to conducting the experiments.

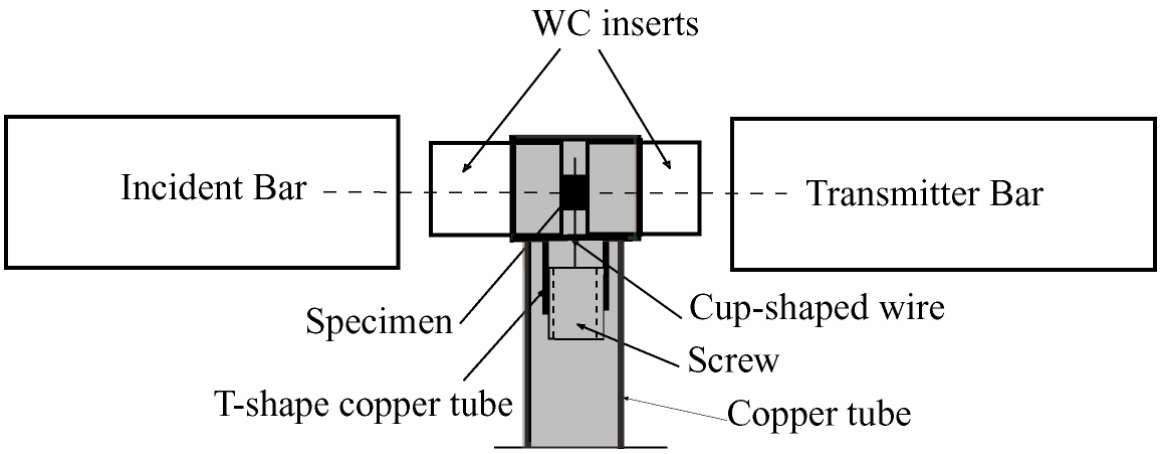

Figure 5: Details of insert-specimen-insert assembly used in the high temperature SHPB tests.

DYNAMIC TENSILE TESTS: SPLIT HOPKINSON TENSION BAR (SHTB)

Although the development of a method to test materials in tension under high strain rate (later called Split Hopkinson Tension Bar, SHTB) was introduced a decade later after the SHPB, the progress in using SHTB was very slow due to difficulties inherent in sample design, load application, and data interpretation. There are five arrangements which have been used to apply a tensile pulse to the specimen. The differences between them inherent in the load application, sample design, and bars arrangement. The historical prospective and the development of SHPB can be found elsewhere (Al Mousawi *et al*., 1997, Nicholas and Bless, 1991).

Figure 7 shows a schematic of the layout of the SHTB at Case Western Reserve University. The SHTB consists of an air operated gas gun, incident bar, transmitted bar, projectile, momentum trap bar, shock absorber, and strain gage circuits to measure the strain signals on the bars. The gun barrel is a 75 mm diameter standard pipe and is 1.33 m in length. It contains a hollow projectile made of hardened 4340 steel. The projectile is equipped with two Teflon pistons and its inner surface, which rides on the incident bar, is honed. The incident and transmitted bars were made of hardened 4340 steel with a RC of 55. The end step of the incident bar (transfer flange) was built by a welding process using 4340 electrodes and was machined to the required size prior to heat treatment. The specimens used in the study were solid bars with threaded ends and a tensile gage section, as shown in Figure 8. The dimensions of the specimen are similar to those employed successfully in the past for SHTB testing (Nicholas, 1981). The specimens were machined from Gamma Met PX bars, and a finish grinding operation was performed over the gage length.

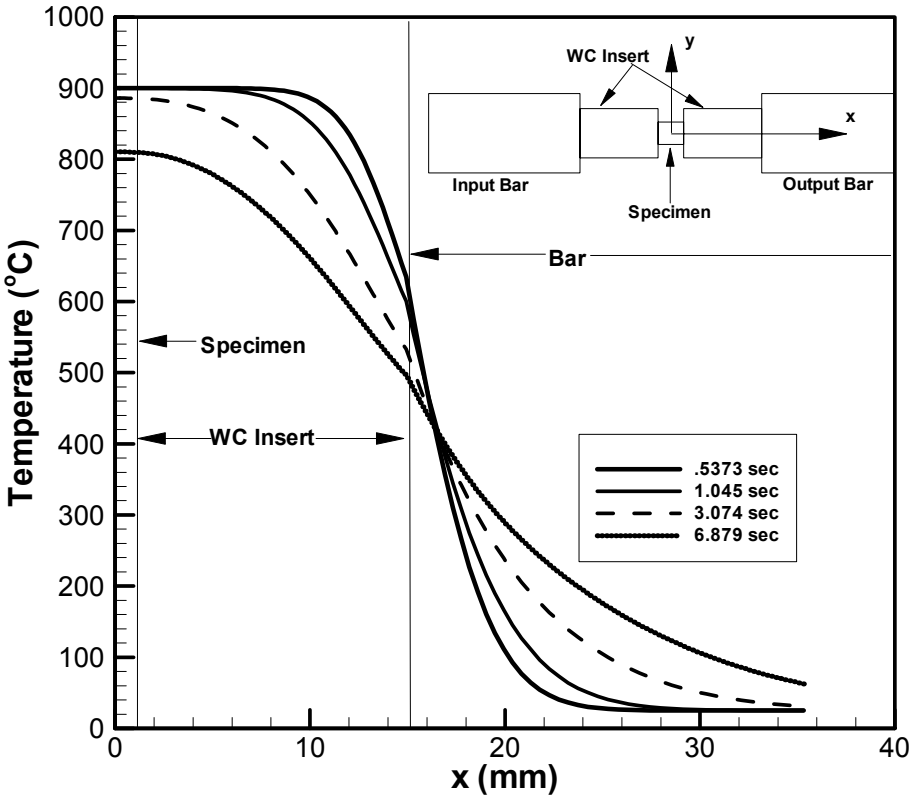

Figure 6: Temperature distribution in the specimen as a function of time.
Note the specimen is sandwiched between two WC inserts.

Prior to conducting the high strain rate experiment, the threaded ends of the specimen were screwed into the input and output metallic bars (these bars are designed to remain elastic during the test). To conduct the experiment the tubular projectile is fired to the right onto to the end step on the right end of the incident bar. A pre-determined gap is kept between the momentum trap bar and the transfer flange such that the end of the momentum trap bar and the face of the transfer flange come in contact once the desired duration of the tensile pulse is transferred to the incident bar through the transfer flange. This tensile pulse then travels towards the specimen, where it is partly transmitted into the transmission bar, and is partly reflected as compression back into the incident bar. In the experiments the impact velocity of the striker bar was varied so as to obtain strain rates ranging from $500s^{-1}$ to $1000s^{-1}$. For all experiments a pulse shaper was utilized on the impact end of the incident bar. A pair of foil strain gages (Measurements Group WK-06-250BF-10C) are strategically attached on the incident while a pair of semiconductor strain gages (BLH SPB3-18-100-U1) are attached on the transmitted bar. These gages are used to record the local strains as the reflected or transmitted pulses pass. The magnitudes and timings of the pulses determine the stress and strain rates in the specimen.

HIGH TEMPERATURE TESTING SET-UP FOR SHTB

With regards to SHTB testing at elevated temperatures, very little previous work exists in the literature (see for example the work by Rosenberg *et al*., 1986). In the present investigation, in order to conduct the elevated temperature tests the ends of the incident and transmitted bars were replaced with impedance matched precipitation hardened Inconel 718 inserts (see Figure 9). The Inconel 718 inserts allow extension of the threaded specimen grips to high temperatures and impedance matching helps to avoid wave dispersion that may occur as a result of a change in mechanical impedance at the 4340 steel and Inconel 718 interface. The specimens were heated using induction heating technique by using a water cooled Hüttinger TIG 10/100 RF generator. This generator uses 3-phase 230-V power line and delivers a maximum power of 10 kW at 100 kHz. The power is coupled to the specimen by using 0.125" copper tubing coils. In the present study, a coil of 0.5" inside diameter and .35" long (two round turns) was used. To avoid damaging the semiconductor strain gages (attached to the transmitted bar) by coil current, the coil was insulated from the bars by using ceramic pieces having 0.125" diameter and 0.5" long. The temperature of the specimen was monitored by thermocouple wires attached to the specimen surface.

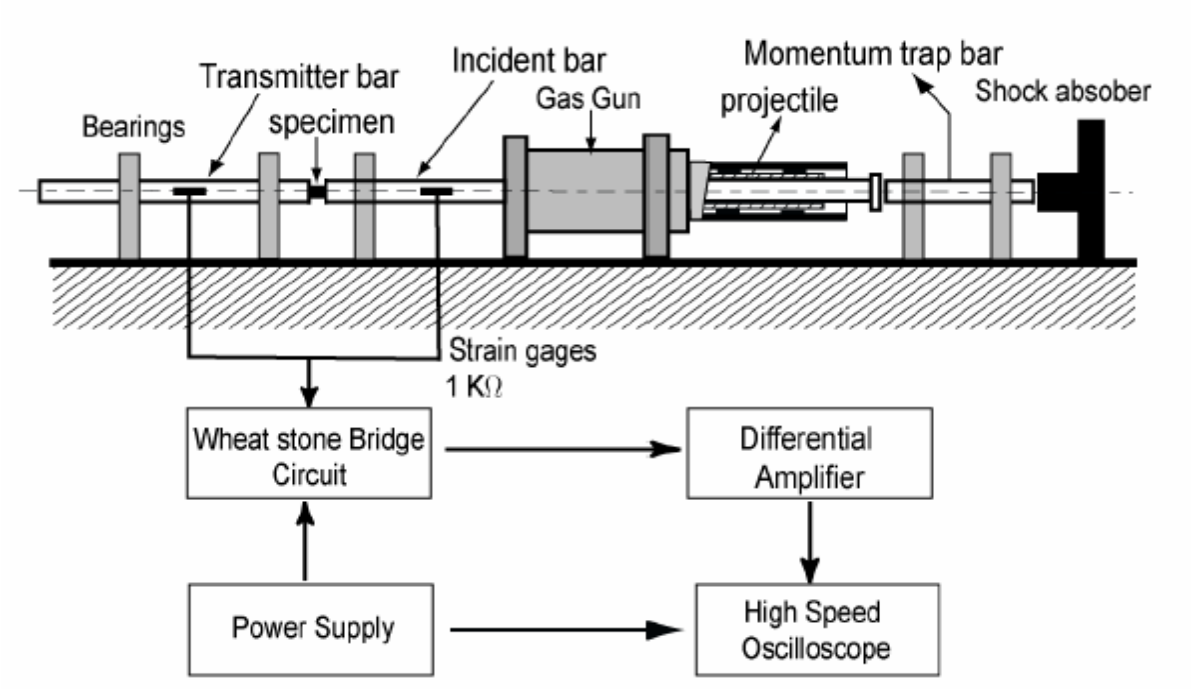

Figure 7: Schematic of Split Hopkinson Tension Bar at Case Western Reserve University.

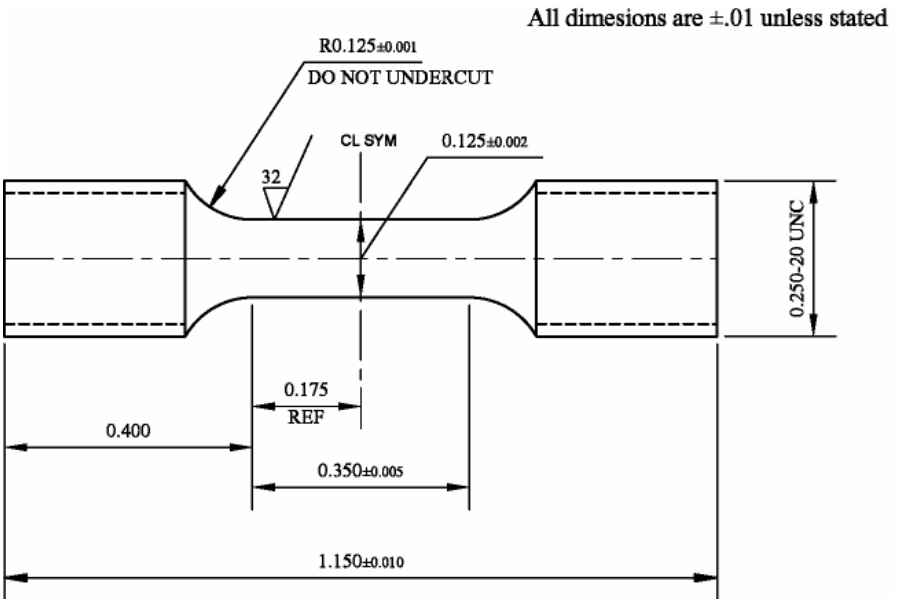

Figure 8: Schematic showing the dimensions of the tensile specimen used in SHTB testing. Please note all dimensions are in inches.

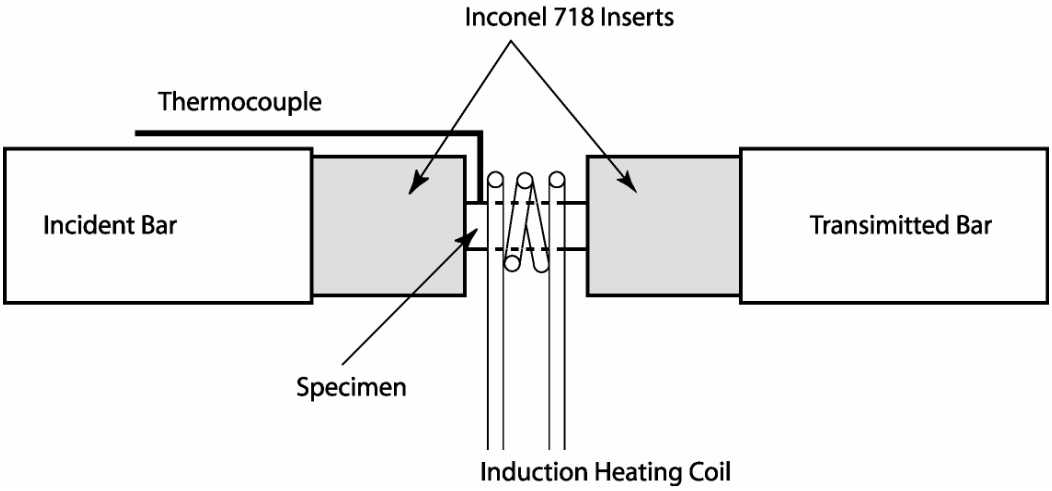

Figure 9: SHTB high temperature set-up used in the present investigation.

EXPERIMENTAL RESULTS AND DISCUSSION

DYNAMIC COMPRESSION TESTING

In order to understand the high strain-rate response of Gamma Met PX a series of dynamic compression tests were conducted using the SHPB facility at CWRU. In these experiments the impact velocity of the striker bar was varied so as to obtain strain rates ranging from 1000 s^{-1} to 3500 s^{-1}. For all experiments a copper pulse shaper was utilized on the impact end of the incident

bar. The pulse shaper aids in dispersing the relatively sharp front of the incident stress wave, and thus allows high-strain-rate experiments to be conducted at near constant strain rates. Also, the slowly rising incident pulse prohibits premature failure of the relatively brittle Gamma Met PX alloys, especially during the early part of stress wave loading.

Figure 10 shows typical incident, transmitted and the reflected strain profiles obtained in typical low impact velocity experiment at room temperature conducted by utilizing a copper pulse shaper. As mentioned before, the transmitted pulse can be related to the strength of the specimen by using Eq. (3), while the reflected pulse is proportional to the strain rate in the specimen (Eq. (2)). The relatively long rise time in the incident pulse is a consequence of the copper pulse shaper. Along with the high-strain-rate tests quasi-static tests ($10^{-2}/\mathrm{s}$) were also conducted to facilitate comparison with the high strain rate data. These specimens were tested using a Shenck Pegasus hydraulic test rig equipped with a 100 kN load cell. The displacement of the samples was monitored using a commercial extensometer.

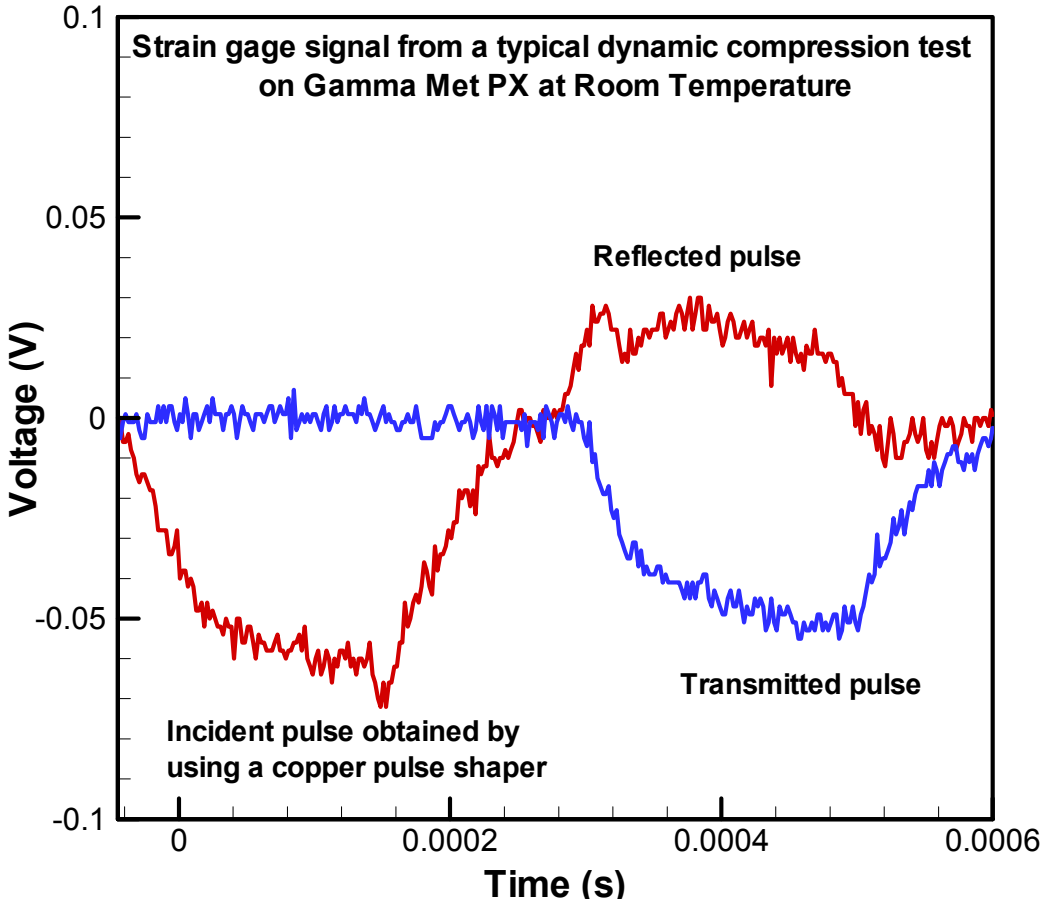

Figure 10: Typical incident, reflected and transmitted strain profiles obtained from a high strain-rate SHPB experiment.

The results of a selected room temperature dynamic compression tests on Gamma Met PX as a function of strain rate are shown in Figure 11. Due to the relatively brittle nature of these alloys true strains of only 0.3 were obtained during the experiments. It is interesting to note the relatively strong strain-rate sensitivity of the alloy at all levels of plastic strain as the strain rate is increased from 0.01 s^{-1} to 3500 s^{-1}. The yield stress of the alloy is approximately 1250 MPa at a strain rate of 0.01 s^{-1} and increases to 2250 MPa at a strain rate of 3500 s^{-1}. Also, the dynamic compressive response shows strain hardening at all levels of strain rates employed in the tests. The test conducted at 3500 s^{-1} resulted in complete failure of the specimen in the form of small fragments. In all the other tests the dynamic compression is stable and does not lead to failure of the specimen.

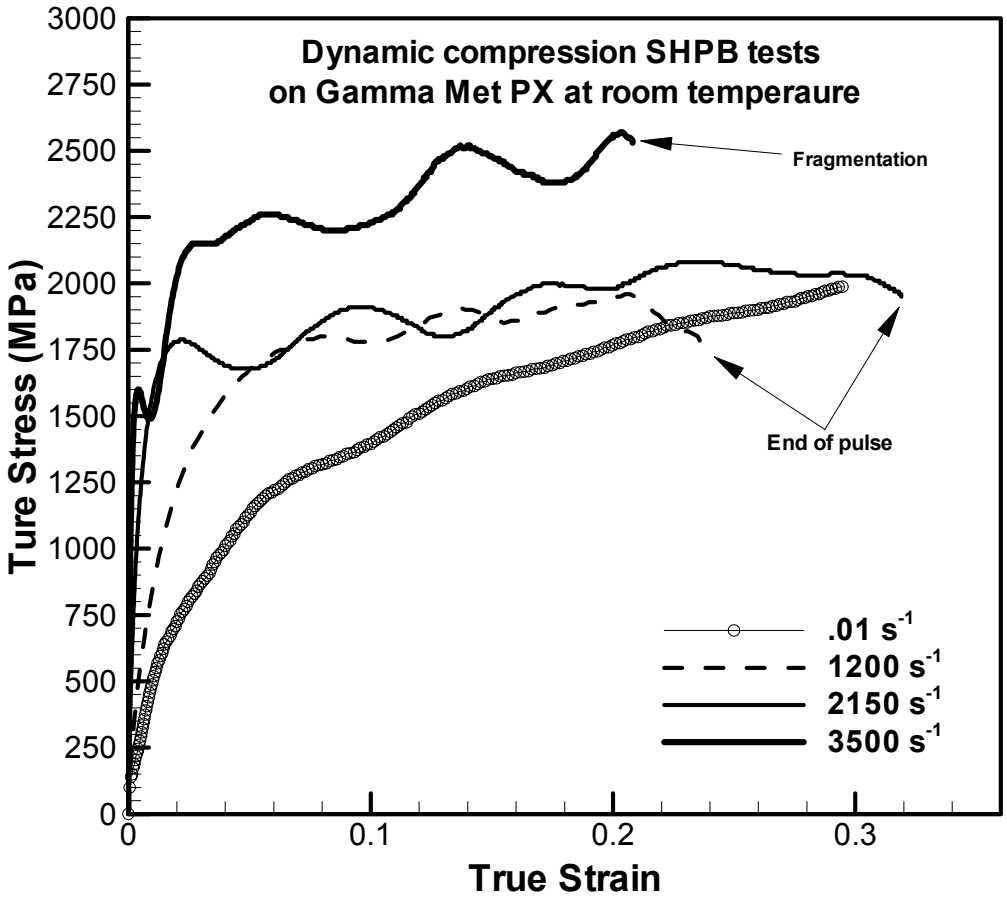

Figure 11: Dynamic compressive response of Gamma Met PX at room temperature as a function of strain rate.

Figure 12 shows the strain gage signals obtained from the dynamic compressive test which resulted in failure during dynamic compression (strain rate 3500 s^{-1}). The incident pulse, the transmitted pulse and the reflected pulse signals are shown. A sudden drop in signal strength is observed in the transmitted pulse at approximately 400 μs. This fall in signal corresponds to a sudden loss in stress carrying capacity of the specimen. The fall in stress is accompanied by a corresponding jump in strain rate, which manifests itself as a sudden jump in the reflected strain pulse signal in the incident bar. After the sudden fall in stress, the strain gage signal in the transmitted bar rises again due to reconsolidation of the crushed specimen in compression.

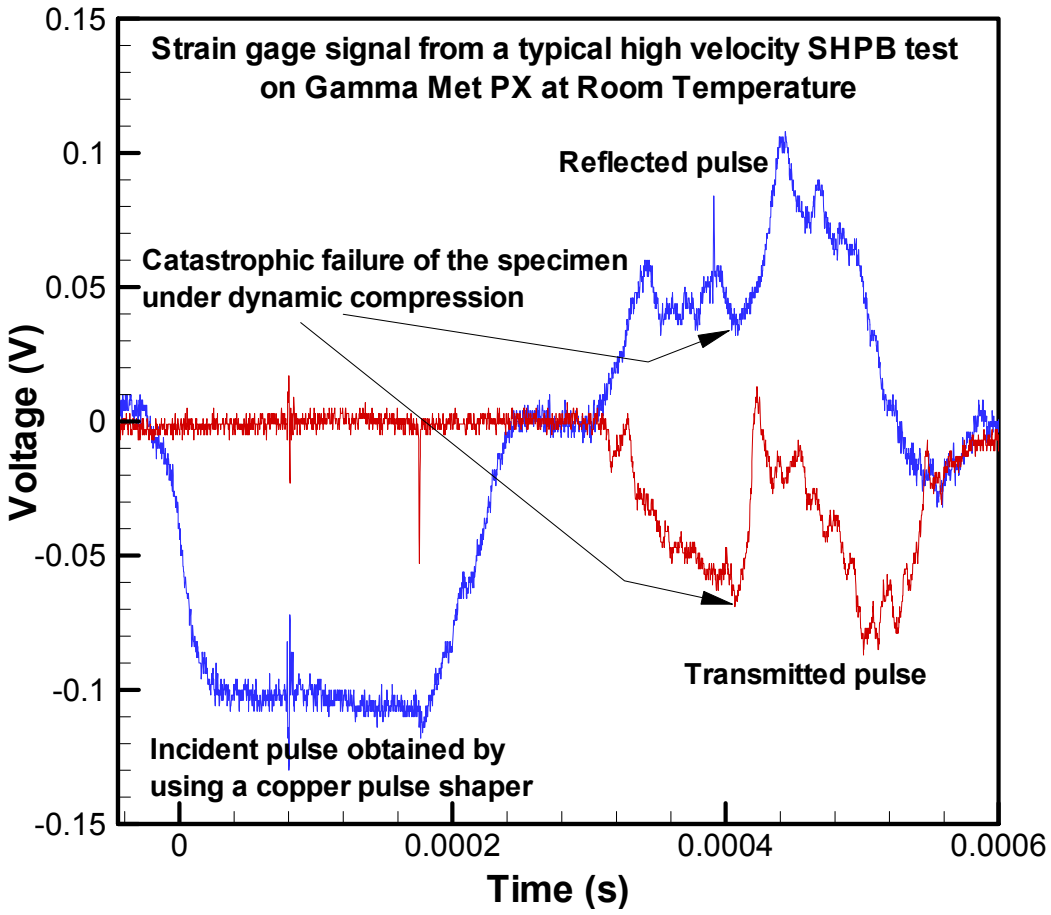

Figure 12: Typical strain gage signal obtained from a relatively high velocity SHPB test on Gamma Met PX showing the failure of the specimen in dynamic compression.

Figure 13 shows four selected frames from a video of a typical high velocity dynamic compression test in which the failure of the Gamma Met PX specimen in dynamic compression was observed. The high speed video was created by an ULTRA 17 camera operating at 150,000 frames per second. The exposure time for each frame is 30 ns. The first frame was acquired after approximately 60 μs of the arrival of the incident pulse at the specimen plane. The progression of damage can be clearly seen in Frame 8. By Frame 10 the dynamic compression of the fragmented specimen is complete and indicates the beginning of the re-consolidation phase of the fragmented specimen.

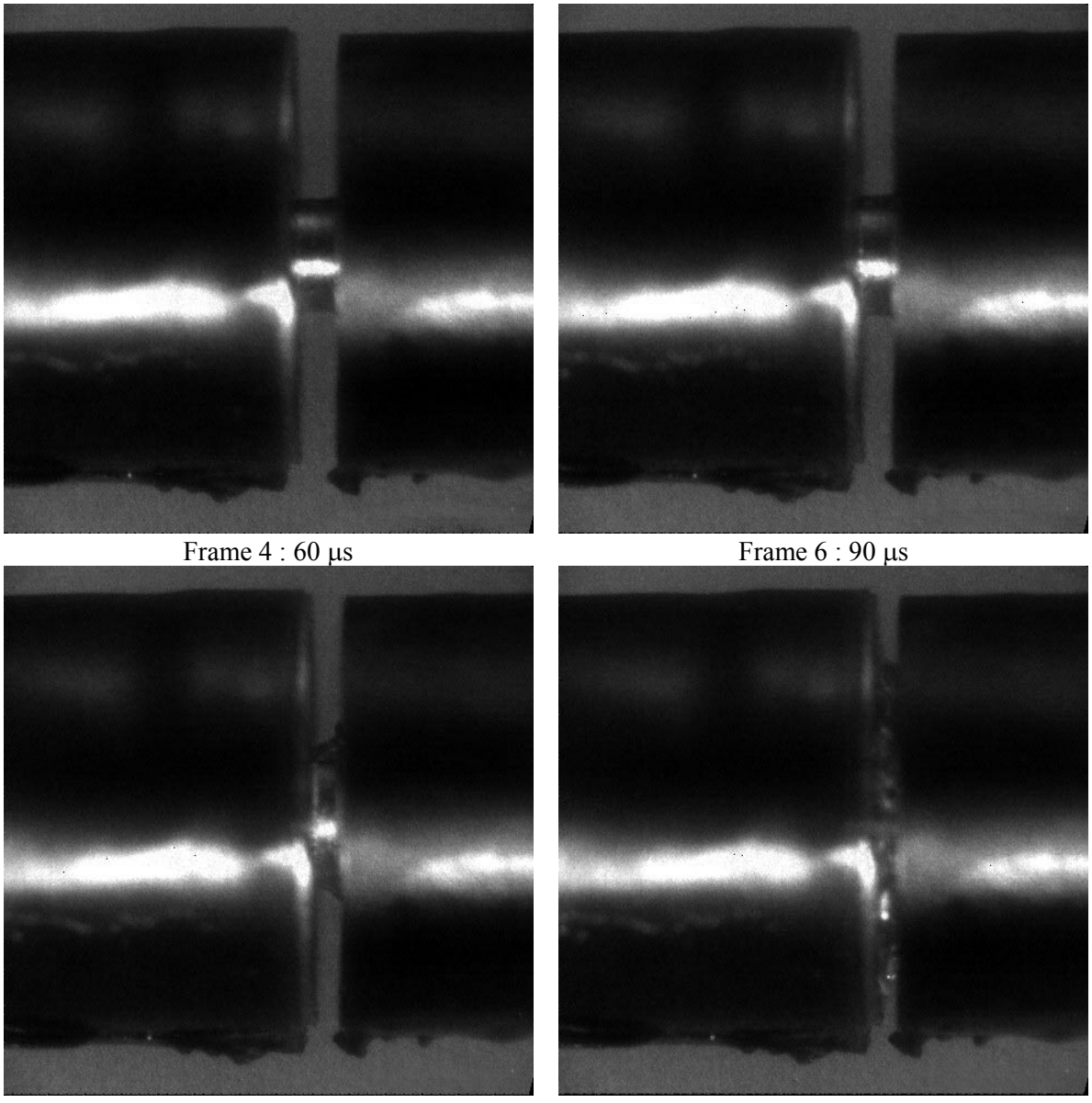

Frame 4 : 60 μs | Frame 6 : 90 μs

Frame 8 : 120 μs | Frame 10 : 150 μs

Figure 13: Shows four selected frames from a video of a typical high velocity dynamic compression test in which the failure of the Gamma Met PX specimen was observed.

Figure 14 shows the dynamic response of Gamma Met PX obtained by the high temperature SHPB facility at CWRU. The dynamic behavior is shown at nominal strain rates of 1800 to 2150 s^{-1}, and temperatures ranging from room to 900 °C. The change in flow stress with temperature is negligible between room temperature and 400 °C. At test temperatures between 600 and 800 °C the flow stress shows signs of thermal softening. Between 800 and 900 °C there is an accelerated drop in the measured flow stress suggesting that the brittle to ductile transition temperature (BDTT) is between 800 and 900 °C. However, the level of flow stress at 900 °C is still higher than those measured for other gamma alloys at the same temperature (Maloy and Gray, 1996; Gardiner *et al.*, 1997). Notice that although the flow-stress levels show thermal softening with increasing temperatures the strain hardening changes very little over the entire

range of test temperatures. Moreover, the strain hardening exponent at elevated strain rates is lower than that observed for quasi-static strain rates at similar test temperatures. This is in contrary to what has been reported for Ti-48-2-2 with duplex microstructure (Maloy and Gray, 1996), where the strain hardening rate increases with increasing the strain rate and remains constant over the whole temperature range.

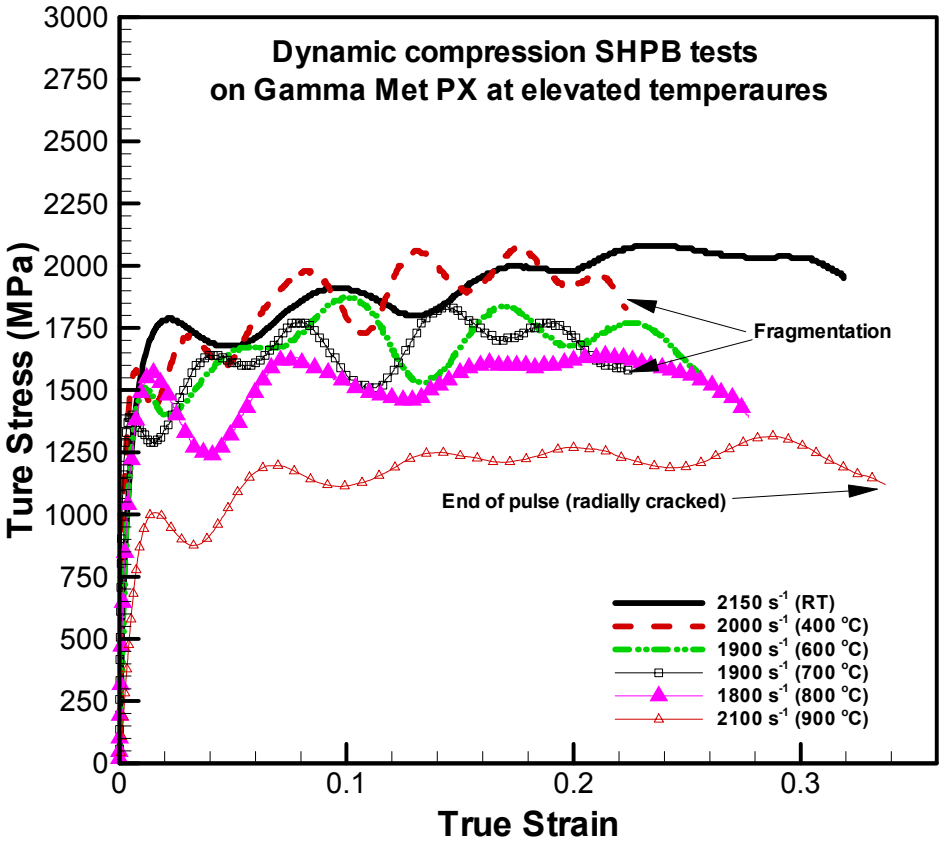

Figure 14: Dynamic compressive response of Gamma Met PX at strain rates of 1800 to 2150 s^{-1} and temperatures ranging from room to 900 °C.

Figure 15 shows the dynamic response of Gamma Met PX at nominal strain rates of 3000 s^{-1} to 3500 s^{-1} and at temperatures ranging from room to 900 °C. At these high strain rates complete fragmentation of the sample is observed to occur during dynamic compression at room, 700 °C, and 800 °C test temperatures. The specimen compressed at 900 °C shows higher ductility and does not fragment. Instead, radial cracking is observed on the specimen after the test. In comparison with Ti-38.5Al-2.7Nb-2.6Mn (Gardiner *et al.*, 1997), Gamma Met PX fractures at lower plastic strain levels at the higher strain rates. However, Gamma Met PX does not fracture at temperatures up to 900 °C while tested at strain rates similar to those of Ti-38.5Al-2.7Nb-2.6Mn, which was observed to fracture at temperatures of 700 °C and higher. These experiments clearly indicate the better ductility of Gamma Met PX with increasing temperature, especially at temperatures beyond 800 °C. Moreover, the alloy does not show any yield anomaly at temperatures up 900 °C, unlike other gamma alloys with similar aluminum content which show yield anomaly at 400 °C (Morris, 1994) or 600 °C (Maloy and Gray, 1996).

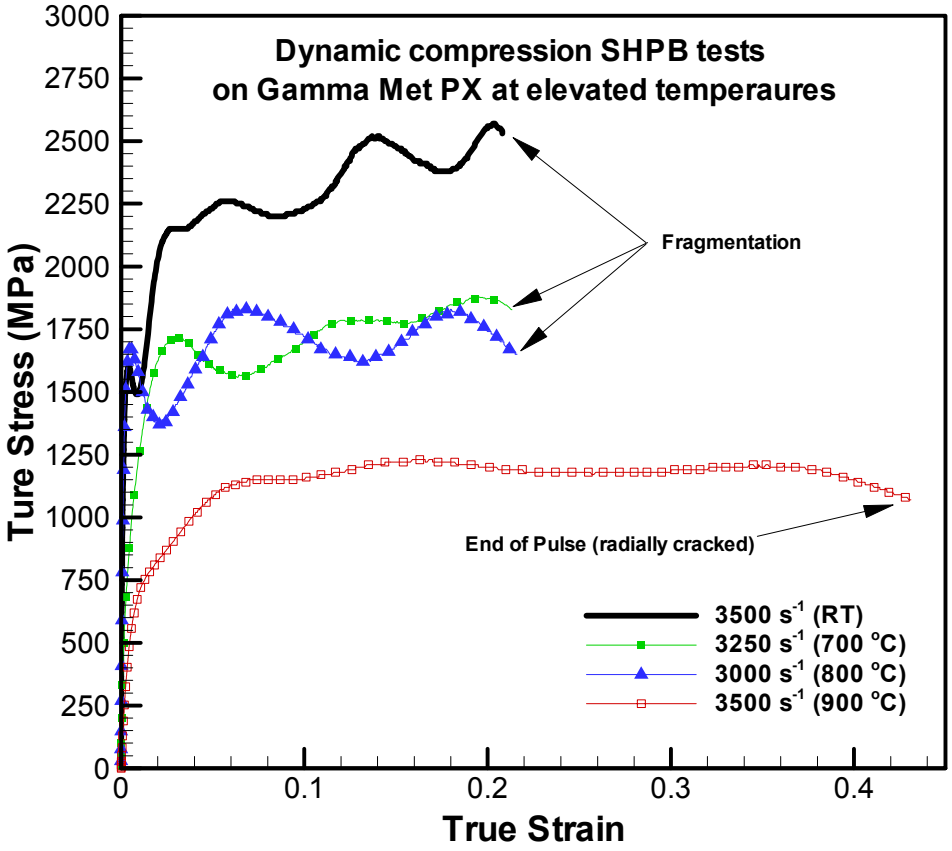

Figure 15: Dynamic compressive response of Gamma Met PX at strain rates of 3000 to 3500 s^{-1} and temperatures ranging from room to 900 °C.

DYNAMIC TENSILE TESTING

To understand the dynamic tensile behavior of Gamma Met PX, the material was tested under strain rate up 1000 s^{-1} and from room to 900 °C. A typical strain gage output for SHTB is shown in Figure 16. The results for selected room and elevated temperatures tests are shown in Figure 17. At room temperature the tensile behavior of the material is observed to be independent of the applied strain rate in the strain rate range 500s^{-1} to 1000s^{-1}. However compared with Ti-47Al-1.5Cr-.5Mn-2.8Nb with duplex and fully lamellar microstructures (Wang et al., 1999a), and Ti-47Al-2Mn-2Nb with nearly lamellar microstructure (Wang et al., 1999b), gamma met PX shows higher strength at failure and similar levels of ductility at similar strain rates. Moreover, Gamma Met PX shows a drop in the yield stress as well as flow stress at all levels of plastic strain with increasing temperature. Also, the strain to failure is observed to increase at elevated temperatures. All specimens were observed to fracture in a brittle manner with the fracture surface remaining essentially normal to the loading direction.

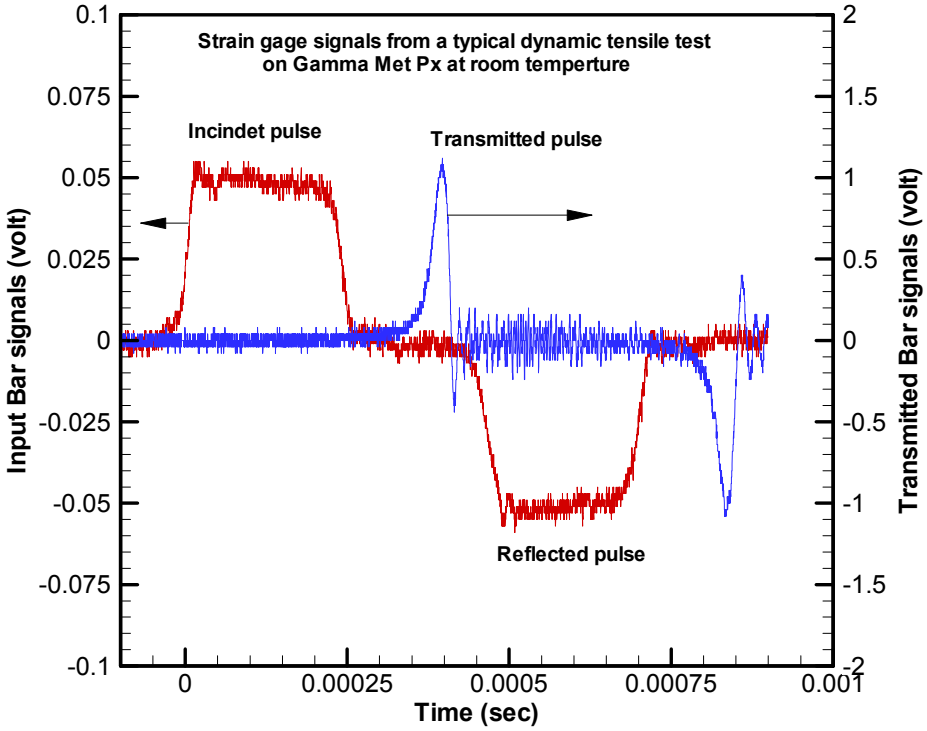

Figure 16: Typical Incident, reflected and transmitted strain profiles obtained from a high strain rate SHTB experiment.

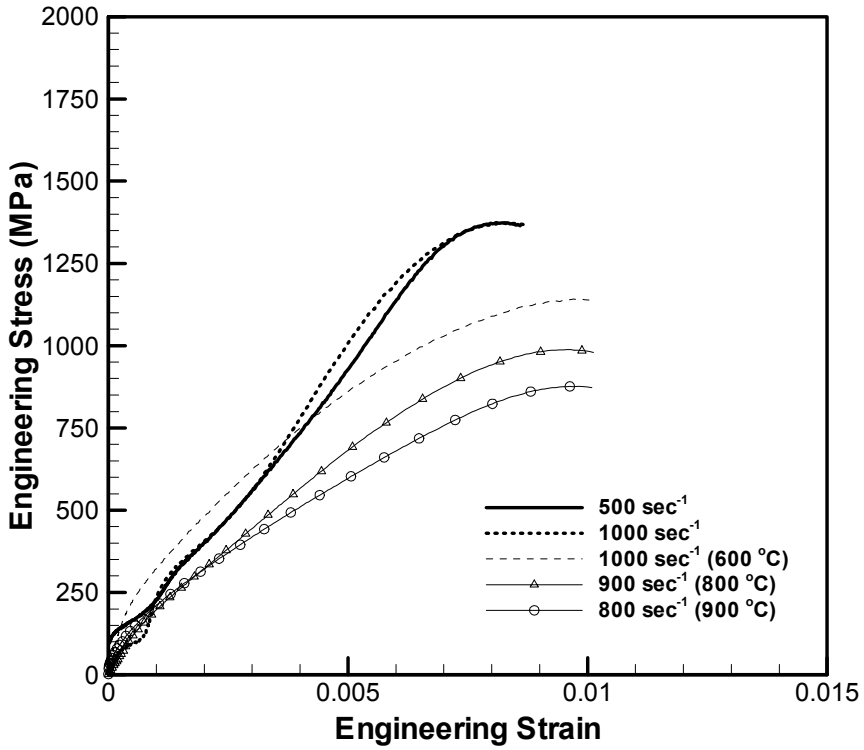

Figure 17: Dynamic tensile response of Gamma Met PX.

CONCLUSIONS

An experimental technique is developed for obtaining thermo-mechanical data for a wide variety of materials in dynamic compression at strain rates ranging from 500 to 3500 s^{-1}. The technique utilizes the use of infra red spot heating devices to heat the specimens, and is relatively simple and economical to integrate with an existing split-Hopkinson pressure bar facilities. For conducting elevated temperature high strain rate tests in tension, an induction coil heating system is utilized. The high heating rates inherent to the spot heating method and the induction coil heating system several of the annealing and ageing issues that are present in other types of furnace configurations are avoided. On the basis of the data obtained to this point, it is clear that these techniques are capable of accurately and repeatedly obtaining elevated temperature data at high-strain rates under both compression and tension.

Using the elevated temperature facility, high-strain-rate thermo-mechanical data is presented for Gamma Met PX under both compression and tension loading conditions and at temperatures ranging from room to 900 °C. Under dynamic compression, the room temperature experiments show that Gamma Met PX is highly rate-sensitive and yield strength as high as 2.2 GPa is observed at strain rates of 3500 s^{-1}. Also, at room temperatures, Gamma Met PX shows appreciable strain hardening at all levels of strain rates employed in the present study. At the elevated temperatures, Gamma Met PX continues to show rate-sensitivity of yield stress and flow stress. The alloy shows little or no thermal softening up to test temperatures of 600 °C and at all strain rates employed in the present investigation. However, at temperatures beyond 800 °C there is an accelerated drop in flow stress. For test temperatures from room to 800 °C and at strain rates in excess of 3000 s^{-1}, the Gamma Met PX specimens are observed to pulverize consistently. However, at test temperatures in excess of 800 °C, the alloy shows better ductility and the failure mode changes from fragmentation to radial cracking. The material does not show any yield anomaly up to 900 °C.

Under dynamic tension (strain rates in the range 500 and 1000 s^{-1}), the room temperature tests show negligible strain-rate dependence on both yield stress and flow stress. Moreover, with an increase in test temperature from room to 900 °C, the material shows a drop in both yield stress and flow stress at all levels of plastic strains. However, the measured levels of failure strength and ductility are higher when compared to those measured for other gamma titanium aluminides, such as Ti-47Al-1.5Cr-.5Mn-2.8Nb and Ti-47Al-2Mn-2Nb, under similar test conditions.

DESIGN AND DEVELOPMENT OF HIGH SPEED PARTICLE IMPACT FACILITY

Graduate Student: David Nathenson

The problem of categorizing impact damage in brittle materials at elevated temperatures and high strain rates is of concern to the aircraft engine industry in their quest for lighter and stronger materials. To this end, a study is being conducted at Case Western Reserve University into the room temperature behavior of impacts on soda lime glass and high temperature investigations of impacts on other brittle materials of interest such as Gamma Met PX and silicon nitride. During the past year the initial phase of this project, the construction and evaluation of a projectile accelerator, was completed.

The actual study consists of three phases. The first of these is evaluation of soda lime glass under high strain rate impact conditions, a material studied extensively under static indentation conditions. Particle impact velocity and specimen thickness are to be varied. This study will yield a comprehensive understanding of internal cracking patterns and stress conditions during dynamic impact. Secondly, examination of Gamma Met PX and silicon nitride subjected to high strain rate impacts at normal and elevated temperatures will occur. Finally, numerical simulation of the impacts will be conducted to facilitate theoretical modeling. The purpose of this study is to gain a comprehensive picture of the material, its stress fields, and the resulting cracking patterns.

Studying these materials under dynamic impact conditions requires the creation of a mechanism to fire projectiles of variable sizes consistently at given velocities. Velocities of between 100 and 300 meters per second are desired to simulate conditions of incoming particles with blades inside of rotating jet engines. Additionally, the front surface target specimen must be oriented to a precise angle to the path of the incoming projectile. The specimens that were chosen for the study are soda lime glass plates of 50mm square with thicknesses of 3, 5, 15, and 25.4 mm. The silicon nitride and Gamma Met PX specimens are disks with radii of two inches and thickness of 1/8 of an inch. Also, the target must be surrounded with a chamber to contain the impact while allowing for observation of the impact and access for heating elements.

PROJECTILE ACCELERATOR DESCRIPTION

In order to accelerate the projectile to the desired velocity, it was decided to utilize an existing design for a split Hopkinson pressure bar firing chamber already in use in our laboratory. This design arrangement allows for a reservoir of high pressure air to build up in a chamber on both sides of a piston (Figure 1). A valve on the back side is then opened to atmosphere, causing the piston to pull back and open the breach. The remaining air in front of the piston then pushes the projectile down the barrel. This firing chamber is designed using one inch thick steel end pieces connected with twelve 5/8 inch diameter bolts to a flanged cylinder. PTFE gaskets seal these pieces. The piston is constructed of aluminum to reduce mass and has two o-rings to provide a seal along its outer rim. Two 1/16 inch diameter holes bored through the piston allow the equalization of pressure between the two sides of the piston during the pressure buildup stage. Filling and firing is accomplished by means of standard plumbing connections.

The gun barrel was designed to use a 3/4 inch diameter sabot and carry it for four and a half feet. This system of sabot and projectile is more effective than using a smaller bore and only the projectile because with a cylindrical sabot, the projectile shape and size can be varied.

A three-quarter inch diameter, 1.5 inch long nylon sabot was chosen (Figure 2). When combined with the actual projectile, in this study a sphere of hardened chrome steel diameter one sixteenth of an inch, the combination masses about 115 grams. The barrel was honed at Commercial Honing and machined with a one inch NPT thread at one end to screw into the firing chamber. This connection, the "breach," is used to load the projectile. In order to separate the sabot from the projectile, a "sabot stripper" consisting of a plate with a 7/16 inch through hole removes the sabot while allowing the projectile to continue unimpeded (Figure 3). The sabot stripper can accommodate particles of any shape and size smaller than 7/16 inches.

The impact chamber contains the aforementioned sabot stripper as well as a target holding apparatus that allows for both angular and linear alignment (Figure 4). The target holder can articulate angularly around the vertical axis and around the horizontal axis perpendicular to the projectile motion using pivots. Linear alignment is carried out by means of screw locked slides that enable the target to be placed precisely in the path of the projectile. The target itself is held in a clamping arrangement that does not impede measurements from the side or from the rear (Figure 5). This device is shaped as a square c-section of metal. The specimen rests against the front of the c section and is supported by the base of the C-section. The back of the holder has a two inch diameter circle machined in it. This circle is used to observe the rear of the specimen. Side observations can also be made because the sides of the holder are open. In this way, the specimen is secured and properly aligned with the path of the projectile. A shelf is included for the placement of optical instruments. The side walls of the chamber are constructed of 1/2 inch steel to prevent shrapnel from escaping. The top, front, rear and portholes in the sides are made of clear shatterproof Lexan to allow for visual measurement techniques.

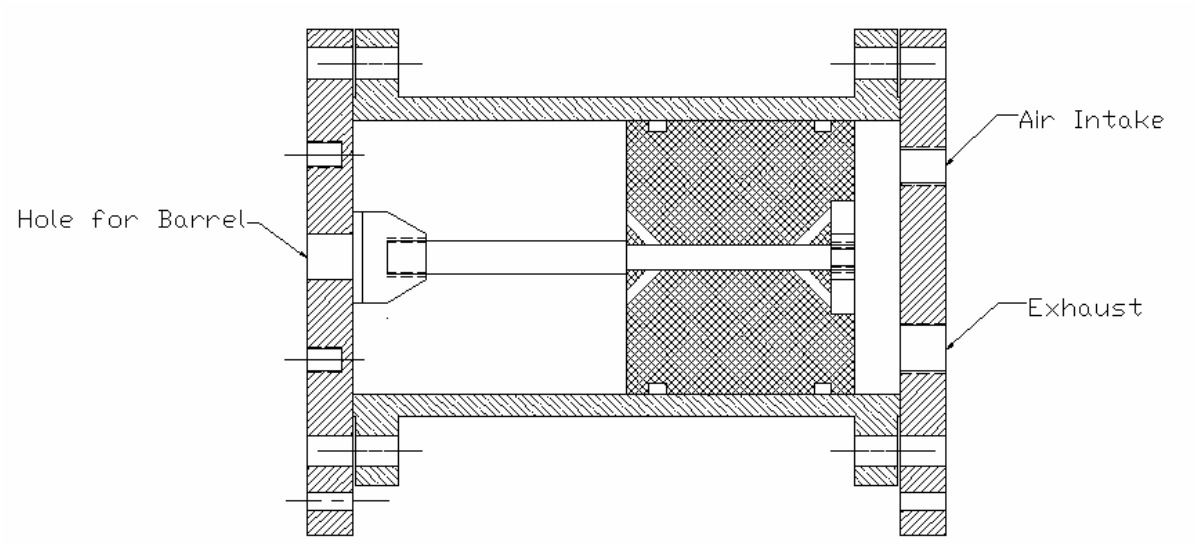

Figure 1: Design of Firing Chamber.

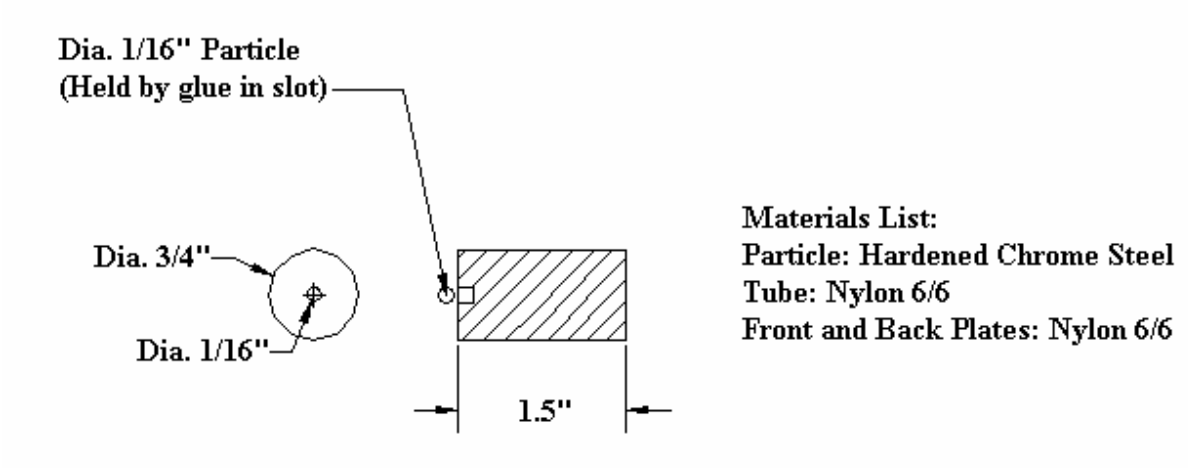

Figure 2: Sabot and Projectile Design.

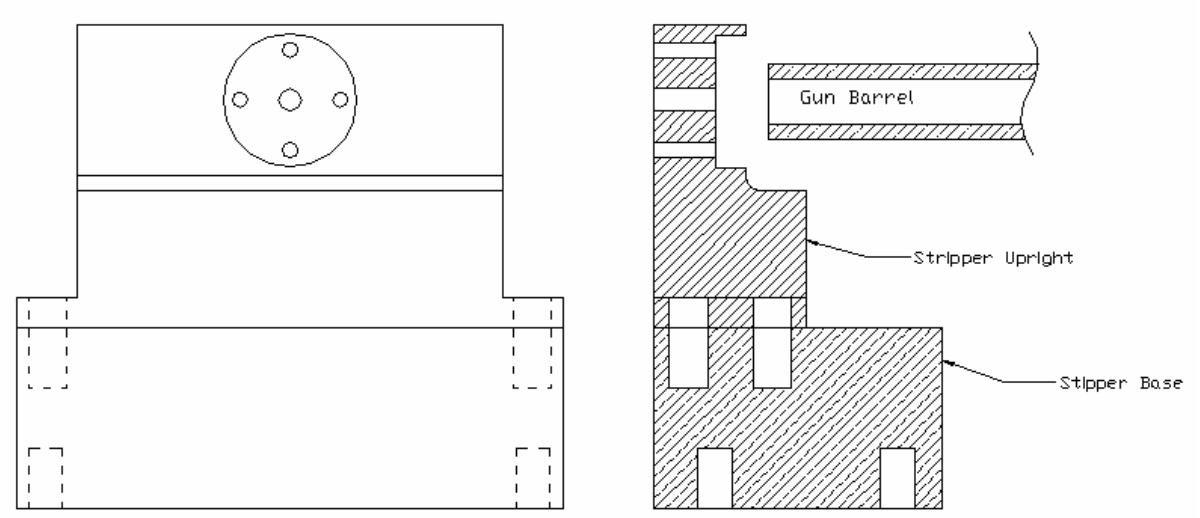

Figure 3: Sabot Stripper Design.

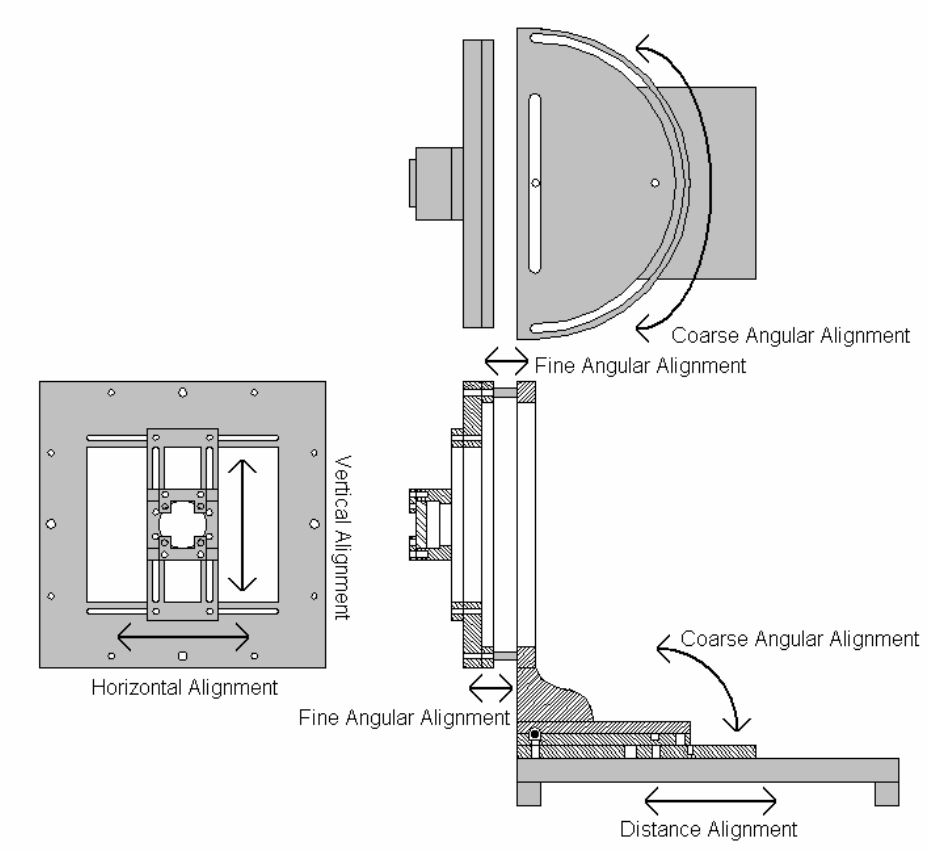

Figure 4: Target Holder – Alignment Systems.

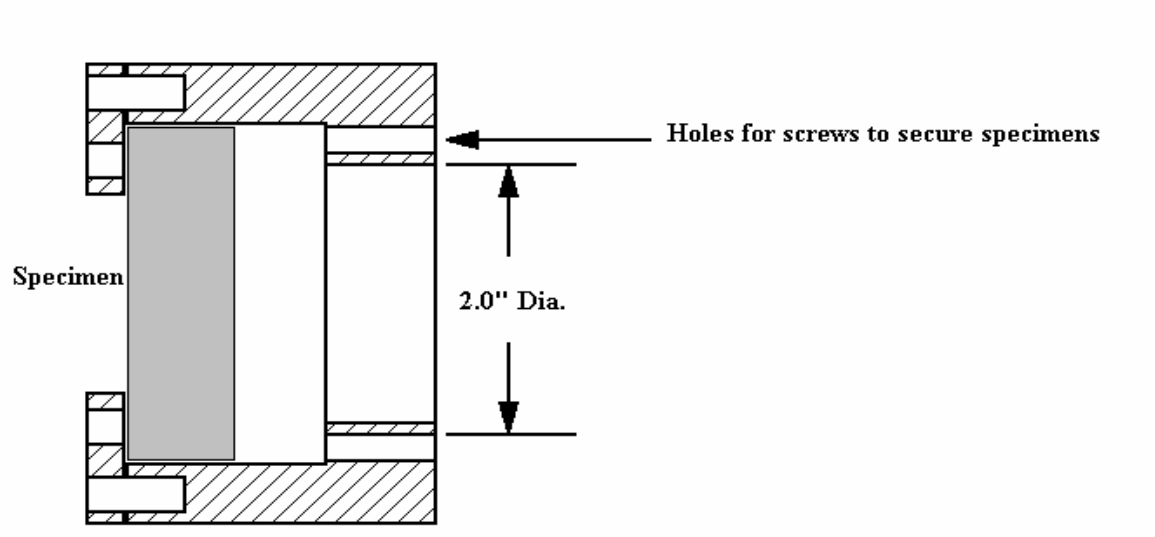

Figure 5: Target Holder – Specimen Holding Section.

OBSERVATION METHODS

Observations of the soda lime glass specimens will be made by four methods: crack pattern investigation by high speed camera, point-wise deformation investigation by VISAR interferometer and strain gauges, and full field deformation by coherent gradient sensing. These systems will be employed in tandem to measure the displacements and strains in the specimens.

DRS Hadland provided a high speed camera that is used to capture the internal crack patterns during the impact. The Ultra 17 camera takes pictures at a rate of up to 150,000 frames per second. That is, one frame every 6.67 microseconds. This allows for comparison to static cracking patterns and the effects of stresses. The frame rate is adjustable to allow for the best capturing of the material behavior. The maximum imaging capacity is seventeen frames. This configuration provides a series of images of the changes in the material.

The VISAR interferometer provided by Valyn International provides point measurements of the out of surface displacement on the rear surface of the specimen. The VISAR probe is used to take point measurements of both the point on the rear surface corresponding to the impact location (the on axis position), and at points off the axis but located at a specific radial distance from the axis. For multiple measurements of neighboring spaces, Valyn VIP provided a multi-beam probe with space for up to seven points. Evaporation coating of the glass specimens provides a reflective surface for the laser beams.

The Coherent gradient sensing provides full field curvature measurements of curvature which can be related to strains. This technique measures the full field of the back surface of the target. The Coherent Gradient Sensing method or CGS was developed by A.J. Rosakis [5]. CGS methods use a laser beam reflected off of the specimen surface and transmitted through a pair of gratings and a lens to produce an image. The beam picks up gradients in the surface curvature which cause fringes when the beams traveling through the gratings interfere with one another.

Strain gauges give a measurement of stresses in both the front and rear surfaces. These stacked tee rosette gages, of type CEA-06-032WT-120, from Vishay Measurements Group, use two perpendicular gages placed one on top of the other in order to get the best point measurement available. These gages are made of constantan alloy with self temperature compensation, 120 ohm resistance, and copper tabs for soldering. Placed upon all of the specimens at a radial position 5mm above the projected point of impact, these gages provide readings of strain very close to the impact location.

With these methods, the state of the deforming material can be completely examined. The silicon nitride and the gamma Met PX specimens will use the same methods, except the internal cracking patterns can not be examined during the test due to the opaque nature of silicon nitride and Gamma Met PX.

PROJECTILE VELOCITY CALIBRATION

The completion of the projectile accelerator paved the way for commencement of the testing phase, but first, the observation system was used to provide a calibration of the loading pressure to firing velocity relationship. The velocity of both the sabot and the projectile were observed. A laser system was used to measure the sabot velocity following its exit from the gun barrel. Also,

the high speed camera was used to provide images of the moving projectile as it exited the sabot stripper. This data was then processed to yield the velocity of the sabot and projectile.

The laser trigger for the camera provided by DRS Hadland is converted into a velocity measurement system by means of a pair of 5mm long cube beam splitters that create two parallel beams, which are projected across the path of the firing sabot. The beams are 5mm apart. This is done despite the slight drop in velocity caused when the impacting particle separates from the sabot at the sabot stripper because the one-sixteenth inch diameter particle is much more difficult to measure with a laser beam than the three quarter inch diameter sabot. The sabot passes through the two beams in sequence and the drop in intensity each time is recorded by means of a high speed photodiode (Figure 6). These drops in light intensity provide accurate velocity measurement.

The high-speed camera is triggered by the above laser system when the first beam is blocked by the passage of the projectile. This laser then triggers the flash and the camera that is set to take exposures of ten nanoseconds duration at the highest frame rate of 150,000 frames per second. This camera takes seventeen pictures which is more than sufficient to establish the velocity. The first exposure begins after a delay determined by the distance between the laser velocity system and the specimen surface, allowing for the recording to commence well before the projectile hits the surface. The images from the camera with the flash backlighting the scene show clearly the projectile exiting the hole in the sabot stripper and hitting the specimen.

A sequence of images taken during a typical impact event is shown in Figure 7. This figure is for projectile velocity of 205 m/s (150 psi). The images represent every third frame taken from the image sequence, thus the approximate time between pictures is 20 microseconds. As can be seen from the images, the impacts cause visible cracking patterns in the specimens and throw up much debris. It should be noted that the same specimens were impacted multiple times during the velocity testing, so cracks already existed prior to the impacts recorded in these sequences.

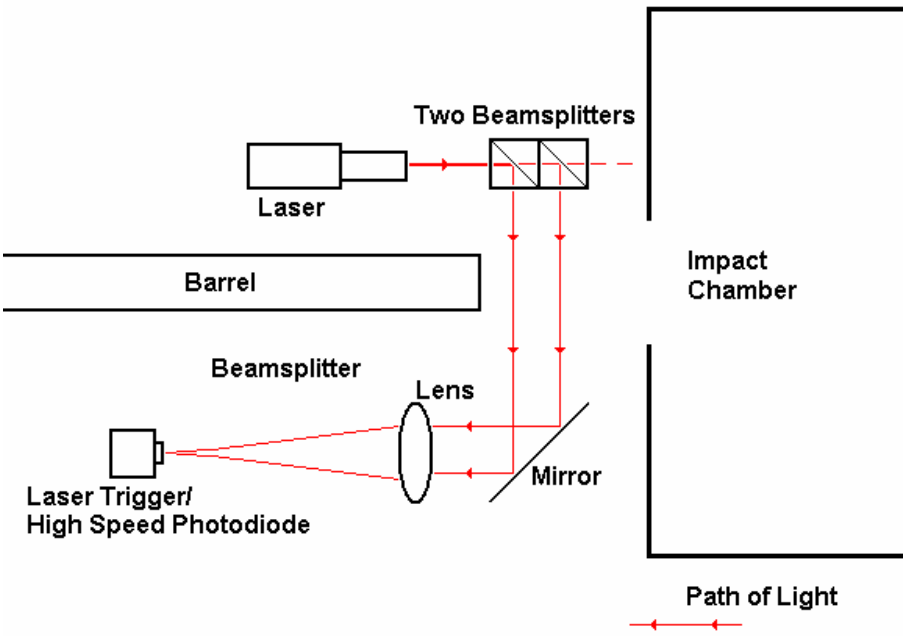

Figure 6: Velocity Measurement System.

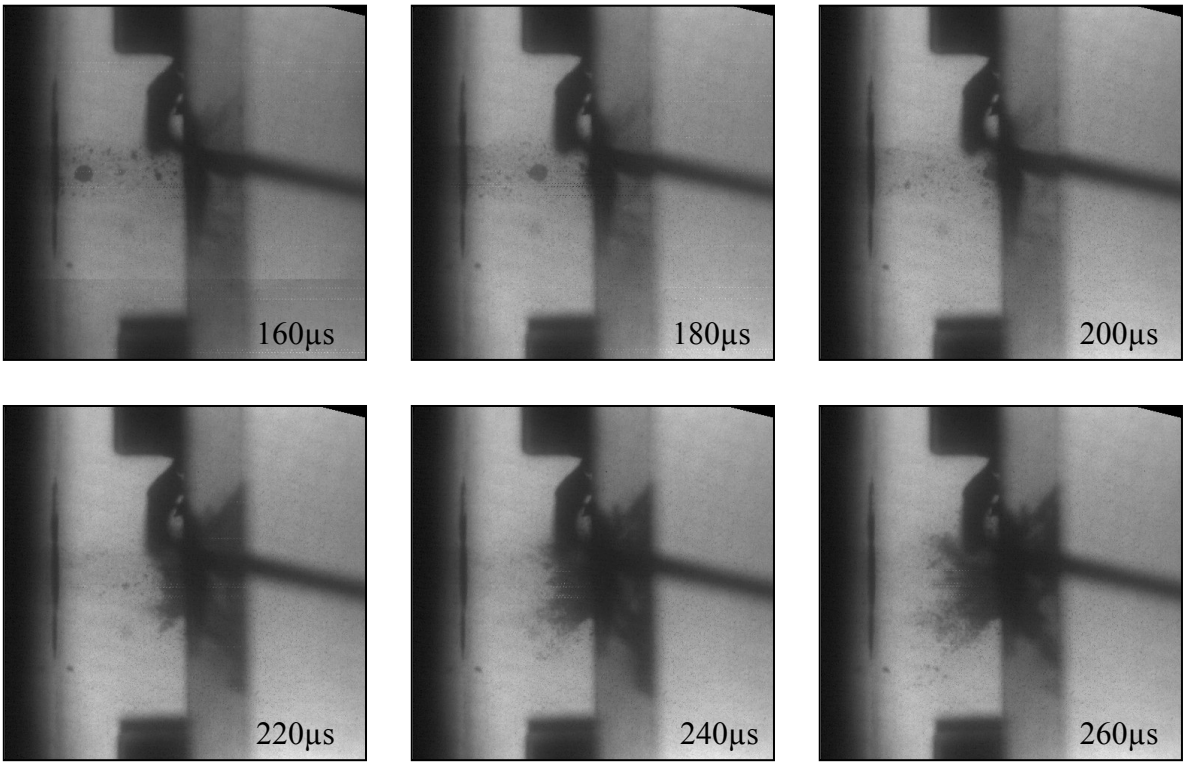

Figure 7: Images of 205 m/s (150psi) test on 5mm thick glass. Shown frames are 20µs apart. Times are after triggering of velocity measurement system. Note conical like behavior of crack.

Calibration of a distance occurs by entering the measurement of an object on one of the frames. For this series, the width of the front prong of the specimen holder was used, whereas, for the actual experiments, a scale will be placed on the specimen. This distance, and the inter-frame time allows the camera's dedicated computer to determine the velocity by selecting one point in space at two different times (two separate frames). This method yielded the curve for sabot and projectile velocity versus firing pressure (Figure 8). Measurements were taken at pressures of 100, 150, 200, 250, 300, 350 and 400 pounds per square inch. As shown, velocities as high as 290 meters per second have been reached. By curve fitting in Microsoft excel, it was determined that the best equations for velocity in terms of pressure were second order polynomials. These equations are listed as follows:

$$v_s = -0.0002 * P^2 + 0.4778 * P + 134.64$$

$$R_s^2 = 0.8779$$

$$v_p = -0.002 * P^2 + 1.4012 * P + 57.451$$

$$R_p^2 = 0.8779$$

With these equations, the necessary pressure for any given velocity can be determined. These calculations paved the way for the first stage of experiments to commence.

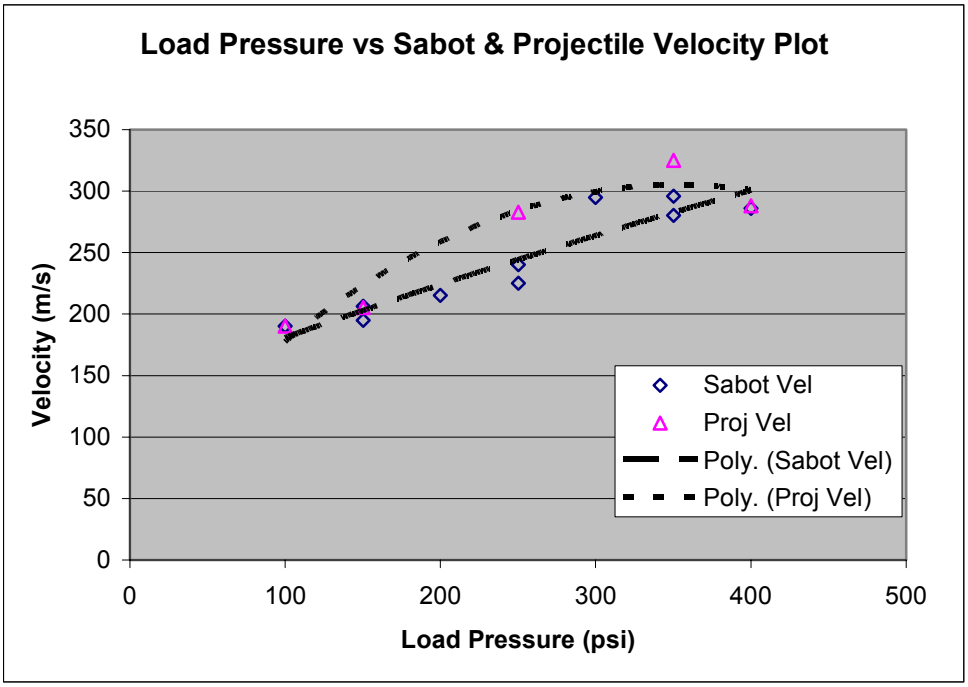

Figure 8: Pressure versus Sabot and Projectile Velocity Calibration Curves.

SUMMARY AND FUTURE WORK

In order to examine the impacts of spherical steel projectiles on brittle materials a gas gun type system was assembled. The system utilizes compressed nitrogen to propel a nylon sabot down a 4.5 foot barrel at speeds up to 300 m/s. Following impact with a sabot stripper, which removes the nylon sabot, the steel projectile impacts the specimen. This specimen, held and aligned by a target holder, is located inside of a protective impact chamber. Laser velocity measurements are taken of every experiment. Several instruments including a high speed camera, strain gages and laser systems record the strains and out of surface displacements of the specimens as well as the cracking patterns.

The laser velocity measurement system and the high speed camera have provided a comprehensive picture of the relationship between the firing pressure of the chamber and the resulting velocity of the sabot and projectile. With this calibration curve, target velocities can be reached consistently. Also, in observing the velocities of sabot versus projectile, it can be seen that little to no energy is lost during the sabot stripping process. This means that the maximum amount of kinetic energy is retained by the projectile following the impact.

Armed with this data, the primary experiments of the soda-lime glass phase are now commencing. Experiments utilizing the VISAR, strain gages, and the CGS method are underway. When completed, this data will serve as a basis for the testing of other brittle materials using the same methods. Specifically, this testing will provide a fundamental understanding of the process of dynamic impact which will be used in the experimental and numeric study of Gamma Met PX and silicon nitride.

REFERENCES

ABAQUS™ Version 6.2-1, Hibbitt, Karlson & Sorensen, Inc., 2001.

Al-Mousawi, M.M., Reid, S.R.; Deans, W.F.; 1997. Use of the split Hopkinson pressure bar techniques in high strain rate materials testing; Journal of Mechanical Engineering Science, 211 (4), 273–292.

Austin C.M., Kelly T.J. and McAllister K.G., 1997. Aircraft Engine applications for gamma titanium aluminides. In: Proceedings of the Second International Symposium on Structural Intermetallics. ed(s): Nathal M.V., Darolia R., Liu C.T., Martin P.L., Miracle D.B., Wagner R. and Yamaguchi M. TMS, Warrendale, PA, pp. 413–425.

Dimiduk, D.M.; Miracle, D.B.; Kim, Y.-W.; Mendiratta, M.G.; 1991. Recent progress in intermetallic alloys for advanced aerospace applications. ISIJ International 31(10), 1223–1234.

Djanarthany, S.; Viala, J.-C.; and Bouix, J.; 2001. An overview of monolithic titanium aluminides based on Ti_3Al and TiAl. Materials Chemistry and Physics 72, 301–319.

Follansbee, P.S.; 1985. The Hopkinson bar. Mechanical Testing, Metals Handbook, Vol. 8., 9 ed. ASM, Metals Park, Ohio, pp. 198–217.

Frantz, C.E.; Follansbee, P.S.; Wright, W.T.; 1984. Experimental Techniques with the SHPB. In: High Energy Rate Fabrication. ed(s): I. Berman and J.W. Schroeder. American Society of Mechanical Engineers, pp. 229–236.

Gardiner, P.; Miguelez, H.; Cortes, R.; LePetitcorps, Y.; Dodd, B.; Navarro, C.; 1997. Dynamic characterization of TiAl intermetallics in hot compression. Journal De Physique IV C3 7, 593–597.

Gray, G.T.; 2000. High strain rate testing of materials: The split Hopkinson pressure bar. Methods in Materials Research. John Wiley Press.

Kaiser, M.A.; 1998. Advancements in the Split Hopkinson Bar Test. MS thesis, Virginia Polytechnic Institute and State University.

Kim, Y-W.; 1989. Intermetallic alloys based on gamma titanium aluminides. Journal of Metals 41(7), 24–30.

Kim, Y.-W.; Dimiduk, D.M.; 1991. Progress in the understanding of gamma titanium aluminide. JOM 43(8), 40–47.

LeHolm, R.; Clemens, H.; Kestler, H.; 1999. Powder metallurgy (PM) gamma based titanium aluminide structures for use in various high temperature aerospace applications. In: Gamma Titanium Aluminides. ed(s): Y.-W. Kim et al. The Minerals, Metals and Materials Society, pp. 25–33.

Lennon, A.M.; Ramesh, K.T.; 1998. A Technique for Measuring the Dynamic Behavior of Materials at High Temperatures. International Journal of Plasticity 14, 1279–1292.

Lui, C.T.; Stiegler, J.O.; Ordered Intermetallics. Metals Handbook. Vol. 2, 10th ed. American Society of Materials, pp. 913–42.

Maloy, S.A.; Gray, G.T.; 1996. High strain rate deformation of Ti-48Al-2Nb-2Cr. Acta Materialia 44(5), 1741–1756.

Millett, J.C.F.; Gray, G.T.; Bourne, N.K.; 2000. Lateral stress measurements and shear strength in shock loaded γ-TiAl alloy. Journal De Physique IV 10, 781–785.

Morris, M.A.; 1994. Dislocation configurations in two phase TiAl alloys III. Mechanisms producing anomalous flow stress dependence on temperature. Philosophical Magazine A 69(1), 129–150.

Nicholas, T.; 1981. Tensile testing of materials at high rates of strain. Experimental Mechanics, 21, 177–185.

Nicholas, T., Bless, S.J.; 1991. High strain rate tension testing; ASM Handbook Vol. 8. 3rd ed., 208–214.

Recina, V.; 2000. Mechanical Properties of Gamma Titanium Aluminides. Report #1577. Chalmers Technical University.

Rosenberg, Z., Dawicke, D., Strader, E., Bless, S.J.; 1986. A new technique for heating specimens in split Hopkinson bar experiments using induction-coil heaters. Experimental Mechanics, 26 (2), 275–278.

Venskutonis, K.R.; 2000. Gamma-met 100 Titanium aluminide sheet production and component fabrication. Preparing for the Future 10(2), 2–3.

Wang, Y.; Dongliang, L.; Kim, Y.-W.; 1999a. High strain rate tensile properties of TiAl alloy in duplex and fully lamellar microstructural forms. Transactions of Non-Ferrous Metals Society of China 9(3), 437–441.

Wang, Y.; Lin, D.; Zhou, Y.; Xia, Y.; Law, C.C.; 1999b. Dynamic tensile properties of Ti-47Al-2Mn-2Nb alloy. Journal of Materials Science 34, 509–513.

Wright, P.K.; 1993. On ductility and toughness requirements for intermetallics in aircraft engines. In: Structural Intermetallics. ed(s): Darolia R. The Minerals, Metals and Materials Society.

Yamagushi, M.I.H.; 1993. TiAl compounds for structural applications. In: Structural Intermetallics. The Minerals, Metals and Materials.

REPORT DOCUMENTATION PAGE

Form Approved
OMB No. 0704-0188

1. AGENCY USE ONLY (*Leave blank*)	2. REPORT DATE	3. REPORT TYPE AND DATES COVERED
	May 2003	Annual Contractor Report—2001–2002

4. TITLE AND SUBTITLE

Modeling of High-Strain-Rate Deformation, Fracture, and Impact Behavior of Advanced Gas Turbine Engine Materials at Low and Elevated Temperatures

5. FUNDING NUMBERS

WU–708–87–23–00
NAG3–2677

6. AUTHOR(S)

Mostafa Shazly, David Nathenson, and Vikas Prakash

7. PERFORMING ORGANIZATION NAME(S) AND ADDRESS(ES)

Case Western Reserve University
10900 Euclid Avenue
Cleveland, Ohio 44106

8. PERFORMING ORGANIZATION REPORT NUMBER

E–13797

9. SPONSORING/MONITORING AGENCY NAME(S) AND ADDRESS(ES)

National Aeronautics and Space Administration
Washington, DC 20546–0001

10. SPONSORING/MONITORING AGENCY REPORT NUMBER

NASA CR—2003-212194

11. SUPPLEMENTARY NOTES

Project Manager, J. Mike Pereira, Structures and Acoustics Division, NASA Glenn Research Center, organization code 5930, 216–433–6738.

12a. DISTRIBUTION/AVAILABILITY STATEMENT

Unclassified - Unlimited
Subject Categories: 01 and 07 Distribution: Nonstandard

Available electronically at http://gltrs.grc.nasa.gov

This publication is available from the NASA Center for AeroSpace Information, 301–621–0390.

12b. DISTRIBUTION CODE

13. ABSTRACT ***(Maximum 200 words)***

Gamma titanium aluminides have received considerable attention over the last decade. These alloys are known to have low density, good high temperature strength retention, and good oxidation and corrosion resistance. However, poor ductility and low fracture toughness have been the key limiting factors in the full utilization of these alloys. More recently, Gamma-met PX has been developed by GKSS, Germany. These alloys have been observed to have superior strengths at elevated temperatures and quasi-static deformation rates and good oxidation resistance at elevated temperatures when compared with other gamma titanium aluminides. The present paper discusses results of a study to understand dynamic response of gamma-met PX in uniaxial compression. The experiments were conducted by using a modified split Hopkinson pressure bar between room temperature and 900 °C and strain rates of up to 3500 s^{-1}. The Gamma met PX alloy showed superior strength when compared to nickel based superalloys and other gamma titanium aluminides at all test temperatures. It also showed strain and strain-rate hardening at all levels of strain rates and temperatures and without yield anomaly up to 900 °C. After approximately 600 °C, thermal softening is observed at all strain rates with the rate of thermal softening increasing dramatically between 800 and 900 °C. However, these flow stress levels are comparatively higher in Gamma met PX than those observed for other TiAl alloys.

14. SUBJECT TERMS

Gamma-met PX; High speed particle impact; Dynamic compression and tension

15. NUMBER OF PAGES

36

16. PRICE CODE

17. SECURITY CLASSIFICATION OF REPORT	18. SECURITY CLASSIFICATION OF THIS PAGE	19. SECURITY CLASSIFICATION OF ABSTRACT	20. LIMITATION OF ABSTRACT
Unclassified	Unclassified	Unclassified	